

CONTRIBUTIONS FROM THE MUSEUM OF PALEONTOLOGY

THE UNIVERSITY OF MICHIGAN

VOL. 27, No. 1, p. 1-50

April 1, 1985

---

**ENAMEL ULTRASTRUCTURE OF MULTITUBERCULATE  
MAMMALS: AN INVESTIGATION OF VARIABILITY**

BY

SANDRA J. CARLSON and DAVID W. KRAUSE



MUSEUM OF PALEONTOLOGY  
THE UNIVERSITY OF MICHIGAN  
ANN ARBOR

CONTRIBUTIONS FROM THE MUSEUM OF PALEONTOLOGY

Philip D. Gingerich, Director

Gerald R. Smith, Editor

This series of contributions from the Museum of Paleontology is a medium for the publication of papers based chiefly upon the collection in the Museum. When the number of pages issued is sufficient to make a volume, a title page and a table of contents will be sent to libraries on the mailing list, and to individuals upon request. A list of the separate papers may also be obtained. Correspondence should be directed to the Museum of Paleontology, The University of Michigan, Ann Arbor, Michigan, 48109.

VOLS. II-XXVI. Parts of volumes may be obtained if available. Price lists available upon inquiry.

CONTRIBUTIONS FROM THE MUSEUM OF PALEONTOLOGY  
THE UNIVERSITY OF MICHIGAN

Vol. 27, no. 1, p. 1-50, published April 1, 1985,  
Sandra J. Carlson and David W. Krause (Authors)

ERRATA

Page 11, Figure 4 caption, first line, should read "(1050X)," not "(750X)."



# ENAMEL ULTRASTRUCTURE OF MULTITUBERCULATE MAMMALS: AN INVESTIGATION OF VARIABILITY

By

Sandra J. Carlson<sup>1</sup> and David W. Krause<sup>2</sup>

*Abstract.*—The nature and extent of enamel ultrastructural variation in mammals has not been thoroughly investigated. In this study we attempt to identify and evaluate the sources of variability in enamel ultrastructural patterns at a number of hierarchic levels within the extinct order Multituberculata. These levels include: 1) different positions on a single tooth; 2) different depths and orientations of a prepared enamel surface; 3) different teeth from a single individual; 4) isolated teeth assigned to a single species; 5) between congeneric species; 6) between genera; and 7) within suprageneric taxa. Nearly all of the specimens examined can be unambiguously characterized by one of two major ultrastructural types: large ( $\bar{X}$  diameter = 8.2  $\mu\text{m}$ , N = 32, sd = 1.36), arcade-shaped prisms or small ( $\bar{X}$  diameter = 3.6  $\mu\text{m}$ , N = 28, sd = 0.77), circular prisms. Consistent variation in these two types appears only at the level of intergeneric comparisons and above; variation in prism size and shape below this level exists, but is negligible relative to the higher order variation. An analysis of prism spacing and density reveals that small, circular prisms are relatively numerous and closely-spaced per unit area while large, arcade-shaped prisms are relatively few and far between per unit area. In general, there is more interprismatic material between circular prisms, despite their small size. We also compared various modes of preparation used to reveal ultrastructural patterns, and the ways in which patterns have been previously characterized and compared.

Our review of Late Cretaceous and early Tertiary multituberculates reveals remarkable consistency in ultrastructural type at the subordinal level. All of the 13 recognized ptilodontoid genera were examined; all but two (*Cimolodon* and *Boffius*) possess small, circular prisms that are numerous and closely-spaced. Twelve of 20 recognized taeniolabidoid genera were examined; all but three (*Neoliotomus*, *Xyronomys*, and *Microcosmodon*) possess large, arcade-shaped prisms that are few in number and widely-spaced. Specimens of the taeniolabidoid genus *Microcosmodon* are unique among multituberculates in having small prisms that are *either* circular or arcade-shaped. All but one (*Viridomys*) of the seven genera currently classified as Suborder *incertae sedis* possess large, arcade-shaped prisms.

<sup>1</sup> Department of Geological Sciences and Museum of Paleontology, The University of Michigan, Ann Arbor.

<sup>2</sup> Department of Anatomical Sciences, Health Sciences Center, State University of New York, Stony Brook.

## INTRODUCTION

Considerable controversy surrounds the use of tooth enamel ultrastructure as a reliable indicator of evolutionary relationships in mammals. Incongruous results obtained by different workers have led many mammalian systematists to be skeptical of the value of ultrastructural data in reconstructing phylogeny. This skepticism arises from uncertainty regarding sources of variability in enamel ultrastructural patterns. Are there observable differences in ultrastructural patterns that vary with depth in the enamel, with location on a single tooth, with different tooth positions in the same individual, between different individuals, etc.? Do the observed differences represent preparation artifacts or real morphological dissimilarities? If the observed differences represent real morphological dissimilarities, at what level in the taxonomic hierarchy can ultrastructural characteristics be useful in phylogenetic analysis, that is, at what taxonomic level can one detect consistent, discrete differences in ultrastructural pattern? Many of these questions have not been addressed in a systematic fashion for any group of mammals.

Frequently, a higher taxon (e.g., an order) has been characterized as having one of three "discrete" enamel ultrastructural patterns, even though very few species assigned to that taxon (in some cases, only one) have been examined. Thus, for example, all Insectivora, Chiroptera, Sirenia, Cetacea, and Tapiridae are thought to possess "Pattern 1"; all Marsupialia, Artiodactyla, and Equidae to possess "Pattern 2"; and all Proboscidea, Pinnipedia, and Carnivora to possess "Pattern 3" (Boyde, 1964, 1971). More recent work, particularly on primates (e.g., Boyde and Martin, 1982, 1984; Warshawsky et al., 1981) and rodents (e.g., Boyde, 1978; von Koenigswald, 1982), has shown that higher taxa are frequently characterized by more than one pattern. Few attempts have been made to identify and evaluate the sources of variability in enamel ultrastructural patterns within other mammalian higher taxa.

This paper presents the results of an analysis of the sources of variability in ultrastructural patterns within a diverse group of Mesozoic and early Cenozoic fossil mammals, the Multituberculata. Multituberculates comprise one of the oldest, longest-lived orders of mammals. They are known from the Late Jurassic to the early Oligocene, and were among the most diverse and abundant mammals in the Late Cretaceous and earliest Tertiary. Multituberculates were small to medium-sized mammals that were probably largely omnivorous (Krause, 1982b) and, at least in North America, arboreal (Jenkins and Krause, 1983; Krause and Jenkins, 1983). They had a highly specialized dentition characterized by a pair of large, procumbent lower incisors and a variably enlarged, blade-like lower fourth premolar. Their distinctive molars have many cusps arranged in mesiodistal rows, hence the name Multituberculata.

The relationship of multituberculates, as a group, to other mammals, is unclear. Likewise, comparatively little is known of the higher-level phylogeny of multituberculates. Multituberculates are usually classified into three suborders: Plagiaulacoidea (3 families, 13 genera), Ptilodontoidea (4 families, 13 genera), and Taeniolabidoidea (3 families, 20 genera) (Figure 1, Table 1). Some authors would also include the enigmatic Late Triassic Haramiyoida as a fourth suborder (1 family, 3 genera) (e.g., Hahn, 1973; Hahn and Hahn, 1983; Sloan, 1979). Relationships between suborders, and generic relationships within suborders, are also not well known. At least 8 genera are currently not assigned to any of the recognized suborders.

Because intra-ordinal relationships within the Multituberculata are so unclear, we initiated a study to evaluate the utility of enamel ultrastructure in studies of multituberculate systematics. Fosse et al. (1973), with the aid of scanning electron microscopy (SEM), demonstrated that multituberculate enamel is prismatic (Figure 2). These results contrast with those of Poole (1967) and Moss (1969), who were unable to detect prisms when examining thin-sections of enamel

TABLE 1 — Tabulation of the multituberculate taxa and specimens examined during the course of this study. The supraspecific classification is that of Hahn and Hahn (1983). Museum abbreviations are as follows: AMNH—American Museum of Natural History, New York; UM—University of Michigan Museum of Paleontology, Ann Arbor; PU—Princeton University, Princeton; UA—University of Alberta Laboratory for Vertebrate Paleontology, Edmonton; IVPP—Institute of Vertebrate Paleontology and Paleoanthropology, Beijing; ZPAL—Institute of Paleobiology of the Polish Academy of Sciences, Warsaw; UCMP—University of California Museum of Paleontology, Berkeley; UW—University of Wyoming, Laramie; SMU—Southern Methodist University, Dallas, Texas

<i>Supraspecific Classification</i>	<i>Species Examined</i>	<i>Specimens Examined</i>	<i>Age</i>	<i>Locality</i>
Suborder Ptilodontoidea				
Family Ptilodontidae				
<i>Kimbetohia</i>	<i>K. campi</i>	P <sub>4</sub> - AMNH 58659 P <sup>4</sup> - AMNH 58540	Puercan Puercan	Tsosie Rincon, NM Tsosie Rincon, NM
<i>Prochetodon</i>	<i>P. cavus</i>	P <sub>4</sub> - UM 77932 M <sup>1</sup> - UM 77932	Tiffanian Tiffanian	UM loc. SC-165, WY UM loc. SC-165, WY
<i>Ptilodus</i>	<i>P. tsoiensis</i>	P <sub>4</sub> - AMNH 59874	Puercan	Tsosie Rincon, NM
	<i>P. wyomingensis</i>	I <sub>1</sub> - PU uncat. P <sub>4</sub> - PU uncat.	Torrejonian Torrejonian	Rock Bench Q., WY Rock Bench Q., WY
		M <sub>1</sub> - AMNH 14501	Torrejonian	Rock Bench Q., WY
	<i>P. new species A</i>	P <sub>4</sub> - UM uncat.	Tiffanian	Douglass Q., MT
	<i>P. new species B</i>	I <sub>1</sub> - UM 64528 P <sub>4</sub> - UM 63112 M <sup>1</sup> - UM 64528	Tiffanian Tiffanian Tiffanian	Cedar Point Q., WY Cedar Point Q., WY Cedar Point Q., WY
Family Neoplagiulacidae				
<i>Ectypodus</i>	<i>E. powelli</i>	I <sub>1</sub> - UM 72046 P <sub>4</sub> - UM 72021 M <sup>1</sup> - UM 72031	Clarkforkian Clarkforkian Clarkforkian	UM loc. SC-188, WY UM loc. SC-188, WY UM loc. SC-188, WY
<i>Mesodma</i>	<i>M. sp.</i>	P <sub>4</sub> - UM uncat.	Lancian	Bug Cr Anthills, MT
<i>Mimetodon</i>	<i>M. silberlingi</i>	P <sub>4</sub> - AMNH 35499 M <sub>1</sub> - AMNH 35499	Torrejonian Torrejonian	Gidley Q., MT Gidley Q., MT
	<i>N. hunteri</i>	P <sub>4</sub> - UM uncat.	Tiffanian	Scarritt Q., MT
<i>Parectypodus</i>	<i>P. lunatus</i>	I <sub>1</sub> - AMNH 80918 P <sub>4</sub> - AMNH 80472	Wasatchian Wasatchian	E. Alheit Q., CO E. Alheit Q., CO
<i>Xanclomys</i>	<i>X. mcgrewi</i>	P <sup>4</sup> - Uncat.	Torrejonian	Swain Q., WY
Family Cimolodontidae				
<i>Anconodon</i>	<i>A. russelli</i>	P <sub>4</sub> - AMNH 35509	Torrejonian	Gidley Q., MT
<i>Liotomus</i>	<i>L. marshi</i>	P <sub>4</sub> - Uncat.	Cernaysian	Cernay, France
<i>Cimolodon</i>	<i>C. nitidus</i>	P <sub>4</sub> - AMNH 57502 M <sub>1</sub> - UA 66233	Lancian Lancian	Altman Blowout, WY Alberta
Family Boffidae				
<i>Boffius</i>	<i>B. splendidus</i>	M - Uncat.	Montian	Hainin, Belgium
Suborder Taeniolabidoidea				
Family Taeniolabididae				
<i>Taeniolabis</i>	<i>T. taoensis</i>	I <sub>1</sub> - AMNH 12924 P <sub>4</sub> - AMNH 12924 M <sup>2</sup> - AMNH 12924	Puercan Puercan Puercan	Barrel Springs, NM Barrel Springs, NM Barrel Springs, NM
<i>Catopsalis</i>	<i>C. joyneri</i>	I <sup>2</sup> - UM uncat. P <sub>4</sub> - UM uncat. M <sub>1</sub> - UM uncat.	Lancian Lancian Lancian	Bug Cr Anthills, MT Bug Cr Anthills, MT Bug Cr Anthills, MT
	<i>P. lucifer</i>	M <sub>2</sub> - AMNH 21724	Lt. Paleocene	Shabarakh Usu, Mong
	<i>Sphenopsalis</i>	<i>S. nobilis</i>	M <sub>2</sub> - AMNH 21719	Lt. Paleocene
<i>Lambdopsalis</i>	<i>L. bulla</i>	M <sup>2</sup> - IVPP uncat.	Lt. Paleocene	China
<i>Kamptobaatar</i>	—	—	—	—

## Family Eucosmodontidae

## Subfamily Eucosmodontinae

<i>Eucosmodon</i>	<i>E. primus</i>	I <sub>1</sub> - AMNH 59999 P <sub>4</sub> - AMNH 58005	Puercan Puercan	Tsosie Rincon, NM Tsosie Rincon, NM
<i>Stygimys</i>	<i>S. kuszmauli</i>	I <sup>2</sup> - UM uncat. P <sub>4</sub> - UM uncat.	Lancian Lancian	Bug Cr Anthills, MT Bug Cr Anthills, MT
<i>Neoliotomus</i>	<i>N. ultimus</i>	M <sub>1</sub> - UM uncat. I <sub>1</sub> - UM 63294 P <sup>4</sup> - UM 65144 M <sup>1</sup> - UM 64553	Lancian Wasatchian Wasatchian Wasatchian	Bug Cr Anthills, MT UM loc. SC-1, WY UM loc. SC-4, WY UM loc. SC-3, WY
<i>Xyronomys</i>	<i>X. sp.</i>	P <sub>4</sub> - UA uncat.	Puercan	Rav W-1, Sask
<i>Bulganbaatar</i>	—	—	—	—
<i>Chulsanbaatar</i>	—	—	—	—
<i>Kryptobaatar</i>	<i>K. dashzevegi</i>	I <sub>1</sub> - ZPAL MGM 1/37 P <sub>4</sub> - ZPAL MGM 1/37 M <sub>1</sub> - ZPAL MGM 1/37 M <sub>2</sub> - ZPAL MGM 1/37	L. Cretaceous L. Cretaceous L. Cretaceous L. Cretaceous	Bayn Dzak, Mongolia Bayn Dzak, Mongolia Bayn Dzak, Mongolia Bayn Dzak, Mongolia
<i>Nemegtbaatar</i>	—	—	—	—
<i>Tugrigbaatar</i>	—	—	—	—

## Subfamily Microcosmodontinae

<i>Acheronodon</i>	—	—	—	—
<i>Microcosmodon</i>	<i>M. conus</i> <i>M. rosei</i>	P <sub>4</sub> - UA 16095 I <sup>2</sup> - UM 71549	Tiffanian Clarkforkian	Roche Percee, Sask UM loc. SC-188, WY
<i>Pentacosmodon</i>	<i>P. pronus</i>	M <sub>1</sub> - UM 72699 P <sub>4</sub> - UM uncat. M <sub>1</sub> - UM uncat.	Clarkforkian Tiffanian Tiffanian	UM loc. SC-143, WY UM loc. SC-165, WY UM loc. SC-165, WY

## Subfamily Buginbaatarinae

<i>Buginbaatar</i>	—	—	—	—
--------------------	---	---	---	---

## Family Sloanbaataridae

<i>Sloanbaatar</i>	—	—	—	—
--------------------	---	---	---	---

## Suborder incertae sedis

## Family Cimolomyidae

<i>Cimolomys</i>	<i>C. clarki</i>	P <sub>4</sub> - AMNH 77182 M <sub>1</sub> - AMNH 77196	Judithian Judithian	Clambank Hollow, MT Clambank Hollow, MT
<i>Meniscoessus</i>	<i>M. robustus</i>	I <sup>2</sup> - AMNH 112575 P <sub>4</sub> - UM 9785 M <sub>2</sub> - UM 9781	Lancian Lancian Lancian	WY Lance Creek, WY Lance Creek, WY

## Family Cimolomyidae?

<i>Essonodon</i>	<i>E. browni</i>	M <sub>1</sub> - UM 42281	Lancian	Bug Cr Anthills, MT
------------------	------------------	---------------------------	---------	---------------------

## Suborder and Family incertae sedis

<i>Allacodon</i>	—	—	—	—
<i>Cimexomys</i>	<i>C. minor</i>	P <sub>4</sub> - UM uncat. M <sup>1</sup> - UM uncat.	Lancian Lancian	Bug Cr Anthills, MT Bug Cr Anthills, MT
<i>Paracimexomys</i>	<i>P. magister</i>	M <sup>1</sup> - UA uncat.	Aquilian	UA loc. MR-20, Alta
<i>Hainina</i>	<i>H. belgica</i>	M <sup>1</sup> - Hin. 01	Montian	Hainin, Belgium
<i>Viridomys</i>	<i>V. orbatus</i>	P <sup>4</sup> - UA 5634	Aquilian	UA loc. MR-8, Alta



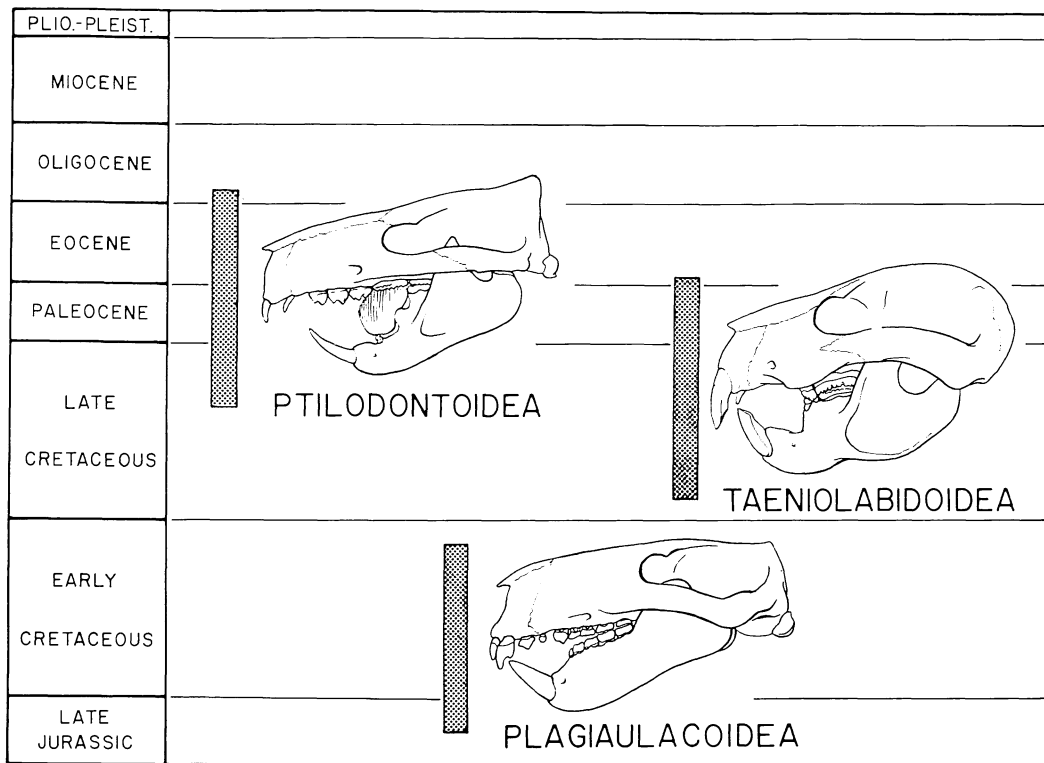


FIG. 1.— Temporal distribution and representative cranial and dental morphology of the three suborders of Multituberculata. Figure from Krause (1982b).

using polarized light (see Osborn and Hillman, 1979). Fosse et al. (1978) later examined a small sample of ptilodontoid and taeniolabidoid multituberculates (two teeth assigned to two species from each suborder) from the Late Cretaceous Bug Creek Anthills locality, Montana. They concluded that: 1) all taeniolabidoids possess exceptionally large enamel prisms and 2) taeniolabidoids can be readily distinguished from all other multituberculates (and, in fact, all other mammals) on this basis.

In order to test the significance of the tentative correlation of large prism size with the suborder Taeniolabidoidea, we increased the sample sizes of both ptilodontoids and taeniolabidoids and investigated other factors whose range of variation is unknown. These other factors fall into two categories: lower levels of variability that can be controlled for in the methodology of the investigator (e.g., preparation technique, location of prepared enamel surface) and those that cannot (e.g., diagenetic effects, previous taxonomic designation). We examined in detail both classes of lower-level variability, because they have the potential to obscure the purported bimodality in size at the subordinal level.

The specific objectives of this analysis, designed, in part, to test the hypotheses proposed by Fosse et al. (1978), are as follows:

- 1) To review the characterization of "discrete" ultrastructural types found in mammalian enamel and, if possible, to develop a useful system for distinguishing ultrastructural types in multituberculates;
- 2) To evaluate the results obtained using various preparation techniques on both fossil and Recent dental materials;
- 3) To investigate variability in enamel ultrastructural patterns in ptilodontoid and taeniolabidoid multituberculates; and
- 4) To provide the necessary information with which to test current hypotheses of ptilodontoid and taeniolabidoid phylogeny; this is the focus of a companion paper currently in preparation.

We demonstrate that it is possible for ultrastructural studies to furnish useful, quantifiable, and reproducible data on dental tissues. We conclude that taxonomic interpretations of ultrastructural data may be developed at a specified level of analysis, but only if all inclusive levels of variability are first investigated.

### CHARACTERIZATION OF ULTRASTRUCTURAL PATTERNS IN MULTITUBERCULATE ENAMEL

Vertebrate tooth enamel is predominantly composed of elongate, hexagonal crystallites of hydroxyapatite. The process of enamel formation (amelogenesis) in mammals results in primarily two fabrics, termed prismatic and nonprismatic. Nonprismatic enamel occurs only in two thin layers; one at the surface of the tooth and the other adjacent to the dentine. Prismatic enamel, which lies between the nonprismatic layers, consists of rods ("prisms") of similarly-oriented crystallites, separated from one another by interprismatic sheets of crystallites (Figure 2). Crystallites making up interprismatic sheets are approximately parallel to one another; the two sets of crystallites (prismatic and interprismatic), however, are usually not parallel. Crystallite orientation can change abruptly and systematically within certain types of prisms; prism boundaries or "sheaths" are thus delineated. Peyer (1968), Boyde (1964, 1971, 1976), Scott and Symons (1977), and Osborn (1981) may be consulted for additional details of enamel structure and development.

Four main categories of characters have commonly been used to characterize and compare mammalian enamel ultrastructure (Figure 2). They concern: 1) prism shape and the nature of prism sheaths, 2) prism size, 3) the spatial arrangement of prisms and the nature of interprismatic material, and 4) the nature of enamel tubules.

*Prism shape and prism sheaths.*—Boyde (1964, 1965) designated three main "repetitive patterns of orientation" of crystallites, referred to simply as Patterns 1, 2, and 3 (Figure 3). Gantt (1982, 1983), following Boyde (1964), attempted to characterize more precisely the range of variation of ultrastructural types and informally subdivided Boyde's original three patterns into seven patterns (1, 2A-C, and 3A-C). These patterns represent a characterization of both the size and shape of individual prisms *and* the two-dimensional array of prisms, as revealed in sections of enamel perpendicular to the long axis of prisms.

We found that, in multituberculate teeth, "ideal" ultrastructural patterns are seldom observed; in particular, the irregular spatial arrangement of prisms obscures the distinction between Patterns 2 and 3 (see below). Because of this difficulty, we characterize prisms as regions defined strictly by the change in orientation of crystallites, in accordance with Boyde (1965), and ignore the highly variable spatial arrangement of prisms. We therefore designate prism type simply as

either circular or arcade-shaped, rather than "Patterns 1, 2, or 3." Circular prisms are those in which the orientation of *all* crystallites in a prism is abruptly different from the orientation of interprismatic crystallites. In contrast, arcade-shaped prisms are those in which the orientation of crystallites on one side of a prism changes gradually, not abruptly (that is, they merge imperceptibly with interprismatic crystallites) (Figure 2B).

Prisms are usually separated from interprismatic material by prism "sheaths." Sheaths are very slight gaps in the crystallite fabric, revealed by the etching process, that are presumably occupied by organic matrix during the life of the tooth. They are best developed along zones where crystallite orientation is most dissimilar. Examination of Figures 11-18 reveals a wide variety in the expression of prism sheaths and in the orientation of prism and interprism crystallites in multituberculates. These differences may be attributable to one or more identifiable factors: variation in diagenetic histories (structural and compositional changes due to fossilization), location and orientation of the plane of section, and response of the enamel to acid etching.

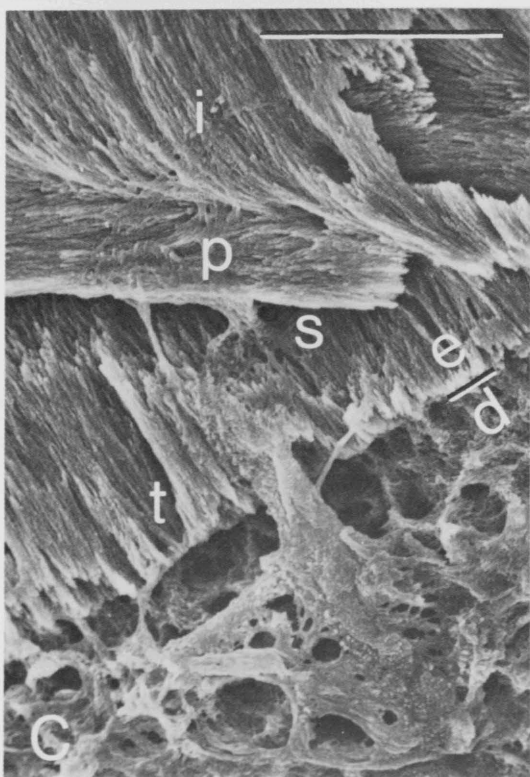
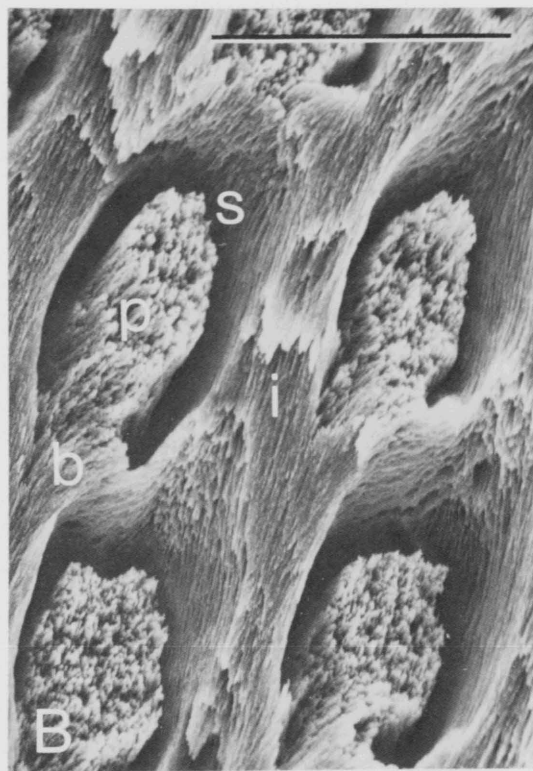
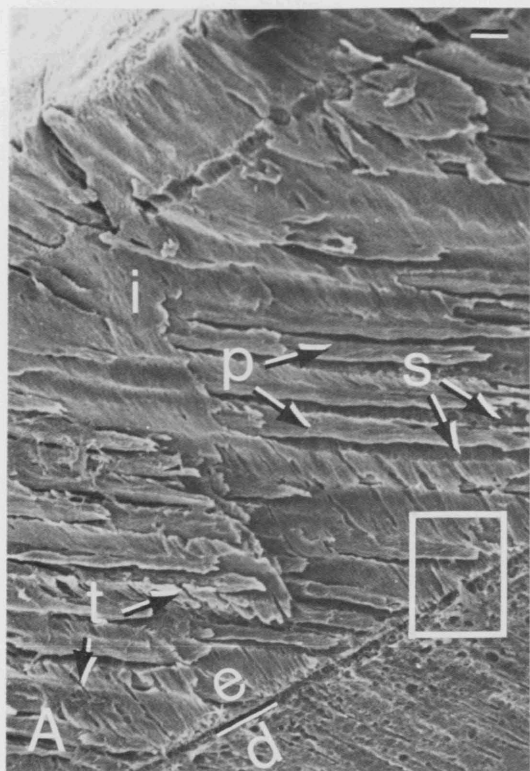
*Prism size.*—There is a consistent correspondence between average prism diameter and prism shape in the multituberculates examined; arcade-shaped prisms are large (average diameter = 8.2  $\mu\text{m}$ ,  $N = 32$ ,  $sd = 1.36$ ) and circular prisms are small (average diameter = 3.6  $\mu\text{m}$ ,  $N = 28$ ,  $sd = 0.77$ ). In our sample, *Microcosmodon* represents an exception in that it has small prisms (average diameter = 4.8  $\mu\text{m}$ ,  $N = 3$ ,  $sd = 0.56$ ) that are either circular or arcade-shaped (see *Variation between genera* for further discussion). It is worth noting that no arcade-shaped prisms as large as 8  $\mu\text{m}$  have been reported, to our knowledge, in non-multituberculate mammals.

A likely explanation for the observed correspondence between prism size and shape concerns the relationship between individual prisms and ameloblasts (Figure 3). Boyde (1965) states that Pattern 2 and 3 (arcade-shaped) prisms are contributed to by two and four ameloblasts, respectively, while a Pattern 1 (circular) prism is associated with only one ameloblast. Nevertheless, in each pattern, there is a one-to-one correspondence between the total number of ameloblasts and prisms per unit area. Boyde (1969) also suggested that the smallest ameloblasts are associated with Pattern 2; Pattern 1 prisms are associated with ameloblasts of intermediate size. Arcade-shaped prisms in multituberculates are much larger than circular prisms, thus indicating that "Pattern 3", and not "Pattern 2", may be represented. However, Boyde's (1965) patterns are defined on the basis of size, shape, and spatial arrangement; the latter characteristic cannot be used with confidence to describe multituberculate ultrastructure (see above). Considering the large size of multituberculate arcade-shaped prisms and assuming that a one-to-one correspondence between the number of ameloblasts and prisms existed in multituberculates (as it does in Recent mammals), ameloblasts in certain multituberculates (those with arcade-shaped prisms) must have been exceptionally large (up to six times larger than in other mammals).

*Spatial arrangement of prisms and interprismatic material.*—Boyde's (1965, 1969) prism Patterns 2 and 3 are distinguished from one another by a difference in size of individual prisms and by the two-dimensional arrangement of prisms. While several workers believe spatial arrangement to be a useful comparative feature of enamel ultrastructure (Boyde, 1964, et seq.; Gantt, 1977, et seq.), we found consistent patterns in multituberculate enamel over very small regions only. Even in apparently clear examples (Figure 4), upon close inspection it is difficult to determine whether prisms are arranged in a regular spatial pattern. This characteristic is too unpredictable to be a standard discriminator of ultrastructural type in multituberculate enamel.

The degree of development of interprismatic material also varies considerably in multituberculates; approximate comparisons may be made between measurements of interprism

FIG. 2— Characteristics of prismatic enamel in multituberculate mammals. (A) Longitudinal section of *Taeniolabis taöensis*, I<sub>1</sub> (250X). Surface of tooth (overexposed) in upper left corner; enamel-dentine junction (e-d) in lower right corner. Occlusal surface of incisor beyond the lower left corner. Total thickness of enamel = 0.34 mm. Prisms (p) inclined at 35° to e-d junction, separated from one another by prism sheaths (s). Interprismatic sheets (i) appear to “blanket” prisms. Tubules (t) run approximately perpendicular to the e-d junction. Outlined region magnified in (C). (B) Close-up (2000X) of four prisms in *Taeniolabis taöensis* I<sub>1</sub> enamel, as seen in a cross-section perpendicular to the section in (A). Surface of the tooth is below the bottom of the photomicrograph; abbreviations as in (A). Note the distinct difference in orientation of crystallites from prism to interprism regions. In these arcade-shaped prisms, crystallites at prism “bases” (b) are continuous from one region to the next; sheaths do not completely isolate prisms from interprismatic regions. (C) Close-up (1600X) of region outlined in lower right corner of (A). (D) Cross-section of *Ptilodus* new species A I<sub>1</sub> (700X). Surface of tooth in upper right corner; enamel-dentine junction in lower left. Total enamel thickness = 0.15 mm. Note change in prism orientation midway through enamel. Prisms in inner portion of enamel are oriented approximately perpendicular to section, and appear artificially elongated; prisms in outer portion are oriented approximately parallel to section. All scale bars (in upper right corners) represent 20 μm.



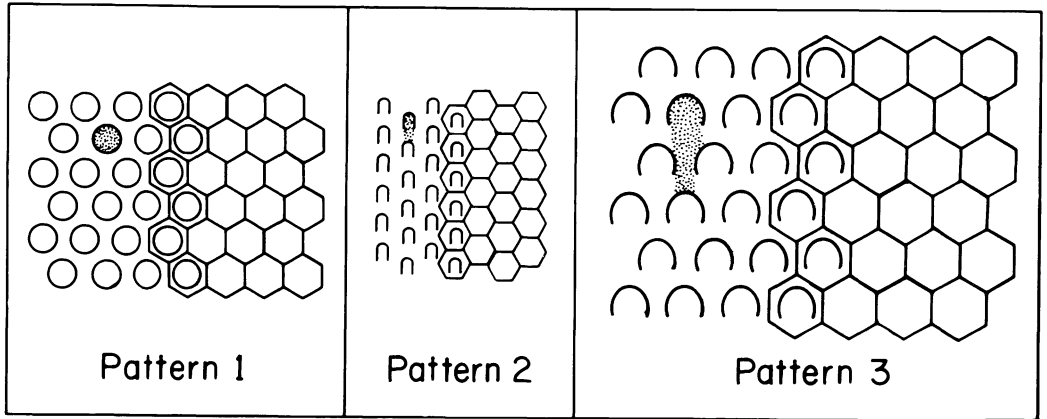


FIG. 3— Schematic representation of Boyde's (1965, 1969) three patterns of enamel ultrastructure. Forty-two prisms of each type are shown illustrating their relative sizes and spatial arrangement in tangential sections through the enamel. Hexagonal outlines represent the secretory territories of individual ameloblasts. Circular or arcade-shaped lines depict prism sheaths. Stippled regions illustrate the area of an individual prism, in each of the three patterns.

spacing and calculations of prism density per  $\text{mm}^2$ . Interprism density, measured between adjacent prism centers, is an approximate characterization of the "packing" of prisms and the relative area of interprismatic versus prismatic material. Multituberculate enamel contains a very large amount of interprismatic material relative to eutherian enamel (Fosse et al., 1973).

*Enamel tubules.*—Enamel tubules appear as small, round holes in the crystallite fabric (see Figures 2A,C and 15C,D). Fosse et al. (1973) noted the presence of tubules in multituberculate enamel. As in marsupials (Boyde and Lester, 1967; Lester, 1971), the tubules appear to be direct extensions of dentinal tubules and occur in interprismatic regions as well as in prism cores (Osborn, 1974; Risnes and Fosse, 1974; see also Fosse et al., 1973; Osborn and Hillman, 1979; Sahni, 1979). Sahni (1979) claims that multituberculate enamel near the enamel-dentine junction contains abundant tubules that are restricted to interprismatic regions, while enamel nearer to the tooth surface contains fewer tubules, restricted to prism cores. Enamel tubules occur in several ptilodontoid and taeniolabidoid genera (Figures 11-18), but their presence or location does not seem to vary in any consistent manner.

#### ANALYSIS OF LEVELS OF VARIABILITY: MATERIALS AND METHODS

To analyze several hierarchic levels of variability in enamel ultrastructure, we examined a total of 64 teeth assigned to 32 of the 41 recognized genera of Late Cretaceous and early Tertiary multituberculates (Table 1, Figure 10). Small ( $1\text{-}2\text{ mm}^2$ ) regions on each tooth were ground,

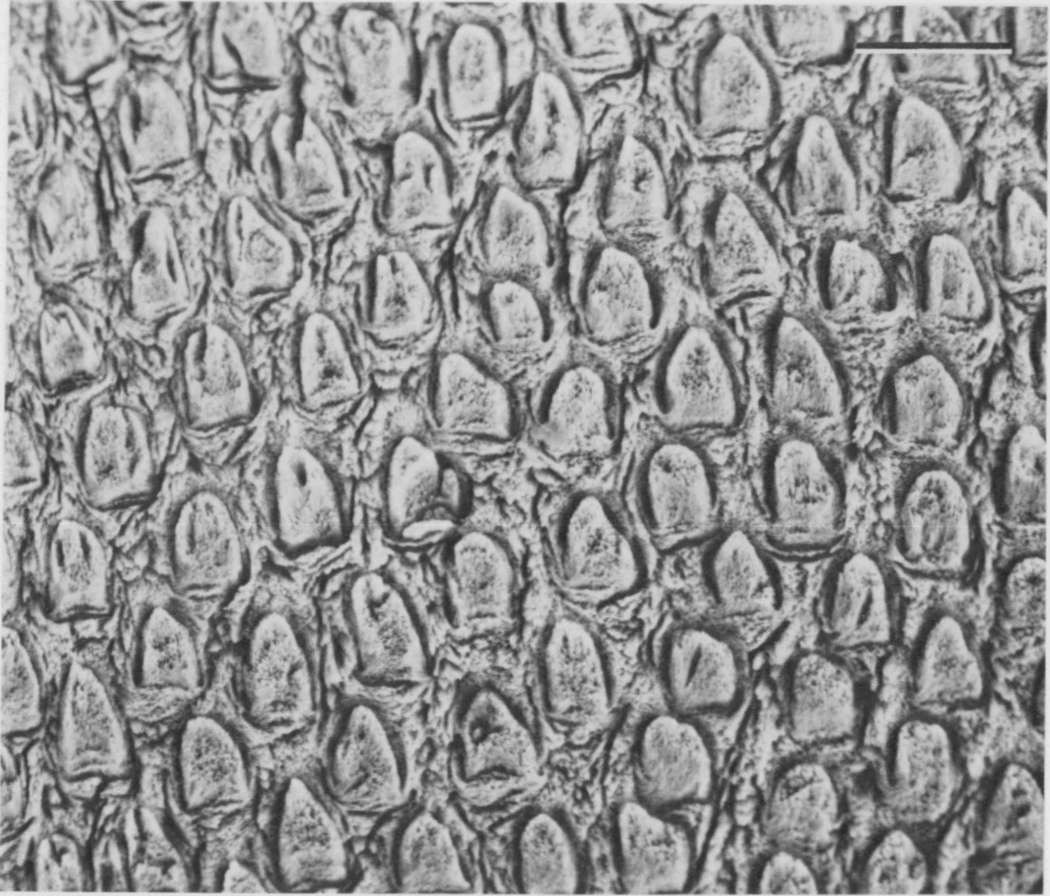


FIG. 4— Tangential section of *Sphenopsalis nobilis* M<sub>2</sub> fragment (750X). The arrangement of prisms appears quite regular, yet close inspection fails to reveal a two-dimensional pattern of prisms consistent with Boyde's Pattern 2 or Pattern 3 (i.e., prisms arranged in vertical columns or horizontal rows). Scale bar = 20  $\mu\text{m}$ .

tangential to the tooth surface, using a slurry of 5.0  $\mu\text{m}$  levigated alumina grit in water. The grinding was carried out under a light microscope, placing a small amount of slurry on the underside of a glass slide and moving the slide gently back and forth over the tooth. Grinding progress could be observed through the glass slide. All grit was removed by ultrasonic cleaning and the teeth were allowed to air dry. Camera lucida drawings of each tooth were made and the prepared region was marked on each drawing. Each tooth was etched for 10 seconds in 5% hydrochloric acid, rinsed, placed in a water bath for 15 minutes to remove any acid residue, and again allowed to air dry. The teeth were then mounted with Duco cement on aluminum stubs and coated with gold in a sputter-coater or vacuum evaporator system, in preparation for SEM examination. The scanning electron microscopes used in this study were a JEOL JSM-U3 (The

University of Michigan) and a JEOL JSM-35C (State University of New York at Stony Brook) both operating at 15 kilovolts.

All measurements of prism diameter and mutual central distance between prisms were made on Polaroid (Type 55 P/N) photographs (Figures 11-18). A standard magnification of 1600X was chosen as a compromise between two conflicting requirements: acquiring the largest sample of prisms per photograph without sacrificing resolution. At this magnification one photograph illustrates between 10 and 30 prisms and provides an adequate sample for measurement. It also has high enough resolution to allow examination of the orientation of individual crystallites, resulting in a more confident determination of prism boundaries.

We performed analysis of variance tests on samples of prism diameters (Figure 10). Each sample consisted of the total number of prisms whose diameter could be measured on each photograph. These statistical comparisons were performed in order to test for significant variation in preparation technique and location of prepared enamel surface, i.e., those levels of variability that are controlled by the investigator (see Introduction).

Since the spatial arrangement of prisms in multituberculate enamel is more irregular than in other mammals and because of difficulties associated with the actual measurement of distances on and between prisms (e.g., obliquity of sections, different effects of etching, etc.), any measurements, and values calculated from them, must be regarded as estimates only. The methods used to calculate these estimates are internally consistent, therefore their value in comparisons within this study is not diminished. Direct comparisons of our results to values given by other authors must be tempered by the realization that slightly different measurements and calculations may have been used. Nevertheless, comparisons can usually be made if the formulae used in the analyses are provided and explained.

An estimate of minimum cross-sectional area per prism (see *Variation in location on a single tooth*) was calculated by squaring the average prism diameter. In most instances, this estimator will produce values that are slightly (artificially) high for circular prisms and low for arcade-shaped prisms. Prism density (number of prisms per mm<sup>2</sup>) was calculated from average mutual central distance (d) between prisms according to the following equation (Fosse, 1968a):

$$\text{Estimate of Maximum Density} = (2 \times 10^6)/(d^2)(3^{1/2})$$

This equation is based on a geometrical distribution of hexagonal closest-packing, which results in a maximum estimate for the number of prisms per mm<sup>2</sup>.

The area of interprismatic material per mm<sup>2</sup> was estimated according to the equation:

$$\text{Interprismatic area} = 1 - (\text{no. of prisms/mm}^2) (\text{min. x-sect. area/prism}).$$

## PREPARATION STRATEGY

Before ultrastructural characters can be described and measured, enamel must be prepared in some way to remove the thin, nonprismatic outer layer and thereby reveal the internal crystallite fabric. Preparation processes potentially alter dental tissues physically and chemically and could cause great variation in ultrastructural pattern. After experimentation with a variety of techniques (Table 2), most workers have adopted methods that involve gentle grinding and/or high speed polishing with very fine (5.0 - 0.5 μm) abrasive grit, followed by short periods of etching in weak acids.



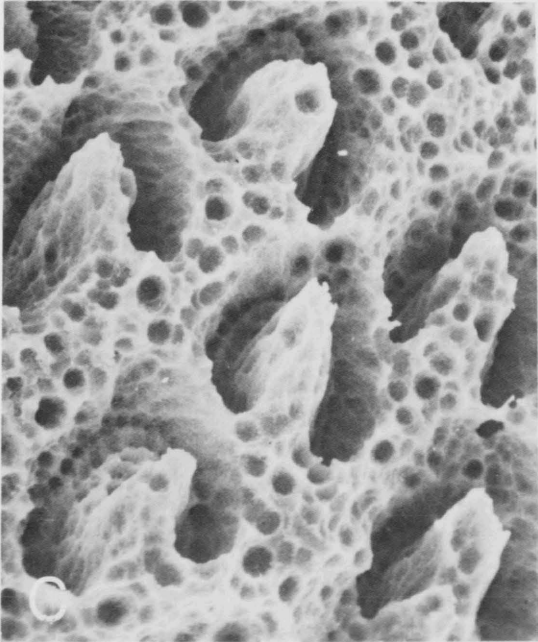
TABLE 2 — Recent examples of the variety of techniques used to reveal enamel ultrastructure.

<i>Acid</i>	<i>Concentration</i>	<i>Etching Time</i>	<i>Material Etched</i>	<i>Reference</i>
H <sub>3</sub> PO <sub>4</sub>	0.5%	60 seconds	Extant primates	Boyde and Martin, 1982
H <sub>3</sub> PO <sub>4</sub>	0.074M (0.5%)	60 seconds	Human premolars	Boyde et al., 1978
HCl	0.01-5M	12 seconds-5 hours	Human premolars	Boyde et al., 1978
H <sub>3</sub> PO <sub>4</sub>	0.074-7.4M	24 seconds-2 hours	Human premolars	Boyde et al., 1978
Lactic acid	0.01-11.4M	2 minutes-60 hours	Human premolars	Boyde et al., 1978
Na <sub>2</sub> EDTA	0.027-0.27M	10 minutes-6 hours	Human premolars	Boyde et al., 1978
Na <sub>2</sub> EDTA	1M	2 minutes-5 hours	Human premolars	Boyde et al., 1978
HCl	5%	5 seconds	Extant and extinct rodents	Flynn and Wahlert, 1978
HNO <sub>3</sub>	2.6%	5 seconds	Cretaceous multituberculates	Fosse et al., 1973
HNO <sub>3</sub>	2%	5 seconds	Cretaceous multituberculates and therians	Fosse et al., 1978
HCl	10%	2.5 minutes	Extant hominoids and Miocene <i>Ramapithecus</i>	Gantt et al., 1977
H <sub>3</sub> PO <sub>4</sub>	0.5%	60 seconds	Neogene hominoids	Gantt, 1979, 1980, 1982
HCl	10%	1 to 4.5 minutes	Triassic <i>Eozostrodon</i>	Grine and Cruickshank, 1977
HCl	10%	60, 90, 120 seconds and 12.4 minutes	Cynodonts and <i>Eozostrodon</i>	Grine et al., 1979
EDTA	0.12 M (pH 7.9)	2, 4, 7, 24 hours	Human teeth	Hoffman et al., 1969
HNO <sub>3</sub>	3%	4 to 20 seconds	Cretaceous multituberculates and therians; Eocene rodents	Sahni, 1979, 1980
HCl	2N (2.2%)	2 to 3 seconds	Extinct and extant rodents	Von Koenigswald, 1982
HCl	10%	2.5 minutes	Extant hominoids and Plio-Pleistocene australopithecines	Vrba and Grine, 1978
HCl	5%	10 seconds	Cretaceous-Tertiary multi-tuberculates	This study

Several recent studies advocate etching teeth for 60 seconds in 0.074 M (0.5%) H<sub>3</sub>PO<sub>4</sub> to reveal prism patterns without creating significant artifacts (Boyde et al., 1978; Gantt, 1979, 1980, 1982; Boyde and Martin, 1982). We prepared three fragments of a single *Taeniolabis taöensis* incisor in three different ways and compared results (Figure 5). One fragment was etched in 5% HCl for 10 seconds, one in 0.5% H<sub>3</sub>PO<sub>4</sub> for 60 seconds, and one in 10% HCl for 2.5 minutes (Gantt et al., 1977; Vrba and Grine, 1978).

Qualitatively, the three patterns resulting from this limited experiment are quite different. Phosphoric acid yielded the least damaging results and 10% HCl for 2.5 minutes the most. Etching with weak phosphoric acid revealed the outlines of prism sheaths, but little else. A 5% solution of HCl for 10 seconds was most effective in revealing the orientation of individual crystallites in different areas. We found this to be a particularly desirable result, because our characterization of prism type depends upon our ability to detect changes in orientation of individual crystallites. The fragment etched in 10% HCl for 2.5 minutes showed artificially enlarged prism sheaths and numerous corrosion pits that totally obscured the orientation of individual crystallites. However, the three techniques did not reveal significant differences in average prism diameter (measured from the centers of the enlarged prism sheaths), as confirmed by an analysis of variance test ( $F_{(1,95)}$ ). Nonetheless, to minimize variability due to preparation artifacts we prepared all specimens in an identical manner (see Materials and Methods) and etched teeth with 5% HCl for 10 seconds. Stronger acids applied for longer times are unnecessarily destructive to the tooth surface and are not recommended. Very weak solutions of HCl and H<sub>3</sub>PO<sub>4</sub> applied for short periods of time produced results that are comparable at the level of analysis utilized in this study.

FIG. 5— Effects of different preparation techniques in revealing enamel ultrastructure (all 1600X; scale bar = 10  $\mu\text{m}$ ). (A) Fragment of *Taeniolabis taoensis* I<sub>1</sub>, etched for 60 seconds in 0.5% H<sub>3</sub>PO<sub>4</sub>. Prism sheaths are distinct; surface less dissected than surfaces revealed by HCl. (B) Another fragment of the same tooth, etched for 10 seconds in 5% HCl. Prism crystallite orientation can be seen to be consistently different from interprismatic crystallite orientation. Interprismatic regions dissected by small “cracks” in enamel fabric. (C) A third fragment of the same tooth, etched for 2.5 minutes in 10% HCl. Sheaths are considerably enlarged at surface; entire surface appears pitted and corroded. Virtually all differences seen between these photomicrographs can be attributed to preparation artifact.



The effects of variable preparation techniques on freshly extracted human teeth have been documented by Boyde et al. (1978) in a comparative study involving several acids of various strengths used for different lengths of time. A similarly thorough study of the effects of etching on fossil teeth with different diagenetic histories would be extremely valuable, but has not been done. It is widely held that "enamel is the only tissue which is virtually fossilized before death" and in which further diagenetic change is negligible (Boyde et al., 1978:991). However, compared to calcium carbonate, the diagenesis of hydroxyapatite is a relatively poorly understood phenomenon. While major structural and compositional changes (clearly evident in  $\text{CaCO}_3$  diagenesis) are not apparent, changes in minor and trace element composition have been reported in fossil bones and teeth (Jaffee and Sherwood, 1951; Parker and Toots, 1970; Fosse et al., 1981). It is possible that these minor diagenetic changes could influence the effects of different etchants.

Examination of 64 multituberculate teeth from a wide variety of depositional/diagenetic environments (Table 1, Figures 11-18) reveals only minor differences in crystallite fabric. No particular diagenetic fabric appears to be consistently associated with a given depositional environment. Minor compositional differences do not appear to cause significant structural changes in the size and/or shape of prisms.

#### ANALYSIS OF VARIABILITY: RESULTS AND DISCUSSION

*Variation in location on a single tooth.*—Prismatic enamel is most accurately characterized from sections cut perpendicular to the long axis of prisms. In order to decide the orientation and position of the most informative section to prepare on any given tooth, it is advantageous to know the orientation of prisms in three dimensions within the entire enamel layer.

Knowing the curvature of the dentine substrate upon which enamel is mineralized during development, the curvature of the completed surface of enamel, and the nature of the process of amelogenesis in mammals, one can predict (to a first approximation) the three-dimensional orientation of prisms. In teeth with relatively "simple" shapes, such as incisors, prisms are oriented in a fairly tight spiral near cusp apices and "relax" to a more open spiral/radial pattern cervically (Osborn, 1968c). Arcade-shaped prisms tend to point toward the occlusal surface and away from the pulp cavity (Figure 2B). Teeth with relatively complex shapes, such as premolars and molars, often have a more complex three-dimensional pattern of prisms within the enamel (Van der Waal and Ripa, 1970; see also Osborn, 1968a,b). This is true for multituberculate teeth as well; they exhibit prisms that change in orientation relative to topographic features such as ridges on the sides of blade-like lower fourth premolars. In general, tangential sections along a relatively flat surface (along the side of an incisor, premolar, or molar) will reveal a more easily quantifiable ultrastructural pattern than tangential sections near the tip of a cusp (Osborn, 1968c).

Because it is common, when dealing with fragmentary fossil material, to have only a portion of a tooth available for study, it is important to know whether the enamel in one region is representative of the entire ultrastructural pattern. This aspect of preparation has not been investigated previously, in a systematic manner, for multituberculate taxa, although Fosse et al. (1978) included drawings that mark the position of the surfaces examined and Sahni (1979) occasionally noted in figure captions which tooth surface was illustrated.

We examined ground and etched tangential sections of enamel at eight positions on  $I_1$  and  $P_4$  of *Ptilodus* new species A and  $M^1$  of *Ptilodus wyomingensis* to determine if any significant differences in ultrastructure exist at different positions on single teeth. We attempted to grind

each section to approximately the same depth at each position. The positions sampled on each tooth are illustrated in Figure 6. No difference in overall prism shape exists from one region to another on the teeth of *Ptilodus*. In other words, all prisms were clearly surrounded by a prism sheath and could thus be identified as "circular," not arcade-shaped. However, depending upon the location sampled, shape varied considerably (from circular to elongate and elliptical) because of the angle of the plane of section through the prism. It is obviously necessary to measure the narrowest dimension of each prism to obtain a minimum value of prism diameter (Fosse, 1968). Analysis of variance tests on samples of prism measurements from all locations sampled on each *Ptilodus* tooth produced significant results at the 95% level.

These results demonstrate that it is critical to select areas on a tooth that will produce a section perpendicular, or as close to perpendicular *as possible*, to the long axes of prisms. Considering the small size of multituberculate teeth, the thinness of the enamel layer, and the manual preparation techniques employed, it is virtually impossible to expect all prepared sections to cut prisms at precisely 90° to their long axes. In the case of the specimens examined here, ventrolingual and ventrobuccal locations near midlength on the crown of I<sub>1</sub>, labial and lingual locations near the base of the crown of P<sub>4</sub>, and labial locations on M<sup>1</sup> are most likely to yield perpendicular sections. An analysis of variance test on three locations on the ventrolabial surface of I<sub>1</sub> was not significant at the 95% level, thus by choosing a subset of locations on topographically similar surfaces, the variation in prism diameter is minimized.

*Variation in depth and orientation of prepared enamel surface.*—The area of the outer enamel surface of a tooth may be as much as twice the area of the inner enamel surface, depending on the thickness of the enamel and topography of the tooth. This difference in area must reflect a corresponding increase in either prism size, prism number, or amount of interprismatic material (or some combination thereof) toward the outer enamel surface. Fosse (1964) documented that prism number does not increase toward the exterior. He reported that the inner surface of enamel contained 10.6% and 7.8% *more* prism bases than the outer surface in Recent human incisor and premolar crowns, respectively. He suggested that a corresponding percentage of ameloblasts "died or disappeared" from the developing front during growth; why this should happen is not clear.

Human enamel, like that of primates in general, is relatively thick; several authors (e.g., Pickerill, 1913; Fosse, 1968b) have shown that the diameter of prisms increases from the enamel-dentine junction towards the outer surface. This has important implications for any comparisons of prism diameter in sections at different depths within the enamel. In their study of multituberculate enamel, Fosse et al. (1978) tentatively suggested that differences between prism patterns on the inner and outer enamel surfaces are not appreciable because multituberculate enamel is thin, compared to enamel of later mammals. In order to test this hypothesis, we examined a series of successively deeper surfaces in the enamel of a *Ptilodus* new species A incisor and a *Taeniolabis taöensis* incisor (Figures 7 and 8). Analysis of variance tests do reveal statistically significant differences ( $F_{.95}$ ) in prism diameters at different levels in the enamel of both *Taeniolabis* and *Ptilodus*. From the tooth surface to the enamel-dentine junction, average prism diameter decreased by 17% in *Ptilodus* and increased by 8% in *Taeniolabis*. These results emphasize the necessity to obtain samples of measurements in the most consistent manner possible. We therefore made every attempt to obtain sections at approximately one-quarter to one-half the distance from the outer enamel surface. In general, the packing of prisms becomes more organized and regular, and the number of enamel tubules (if present) decreases as one proceeds from the enamel-dentine junction to the surface of the tooth, as Osborn (1974) reported for *Didelphis* enamel.

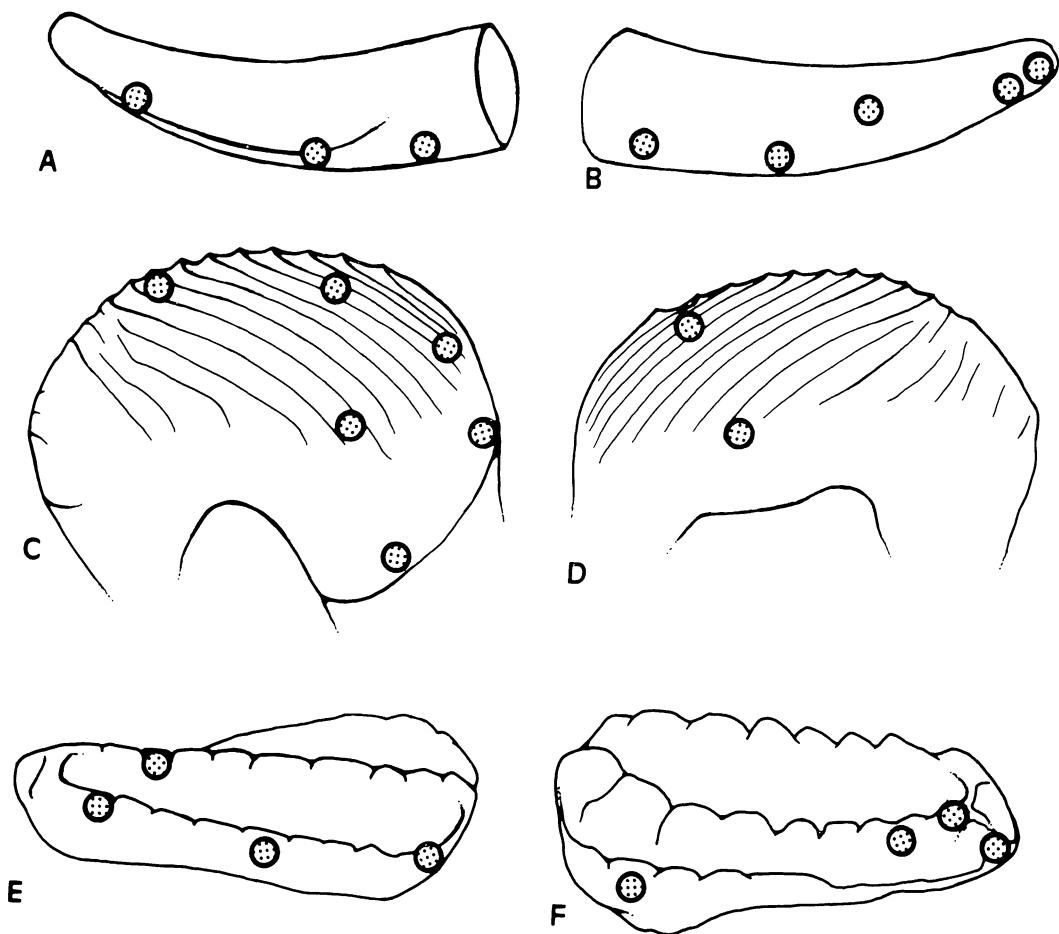


FIG. 6— Positions sampled to examine variation in enamel ultrastructural patterns on single teeth. (A) and (B) Medial and lateral views of right  $I_1$  of *Ptilodus* new species A. (C) and (D) Buccal and lingual views of right  $P_4$  of *Ptilodus* new species A. (E) and (F) Ventrobuccal and ventrolingual views of right  $M^1$  of *Ptilodus wyomingensis*. Each tooth was sampled at eight different positions (indicated by stippled patches).

The three-dimensional orientation of the ground and etched surface within the enamel will certainly affect the dimensions of prisms revealed on that surface. In longitudinal sections through the incisor of *Taeniolabis* (Figure 2A and C), prisms emerge from the enamel-dentine junction at approximately  $35^\circ$  and curve to meet the surface at about  $70^\circ$ . The prisms remain parallel to this section along most of their length. Any section ground tangential to the surface of the tooth will reveal an accurate prism width, but prism length may be artificially elongated by up to 70% (see Fosse, 1968a,c; Fosse et al., 1973:142). This artifact of orientation of section can be seen in other taxa as well (Figures 11-18). Circular prisms appear oblong and arcade-shaped prisms appear considerably longer than wide. As noted in the previous section, when comparing prism diameters it is critically important to measure the narrowest dimension exposed on a surface in order to minimize errors due to distortion of prism outline.

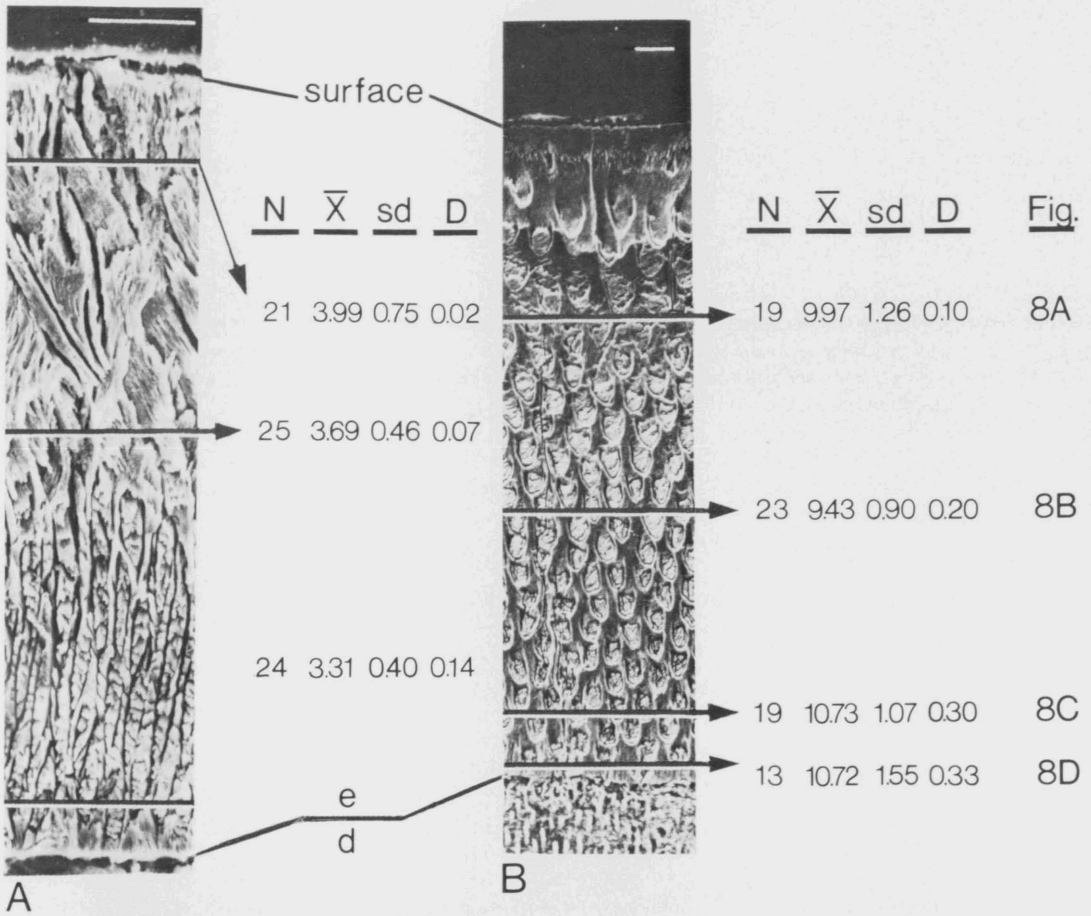
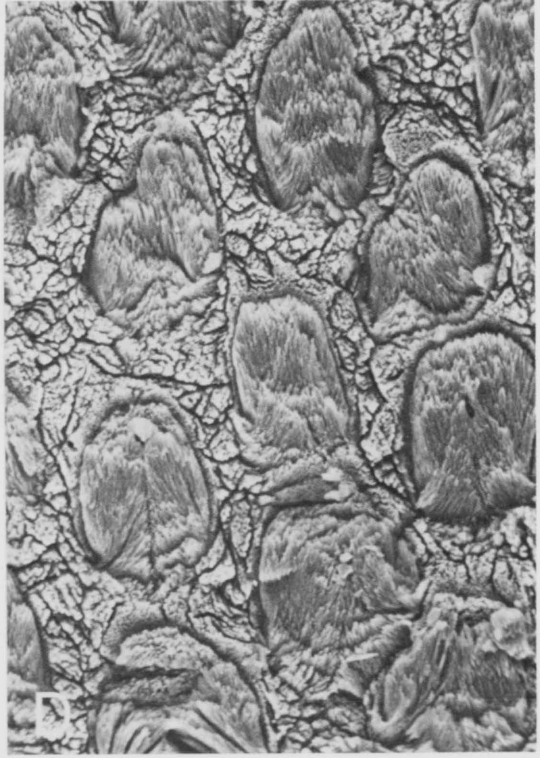
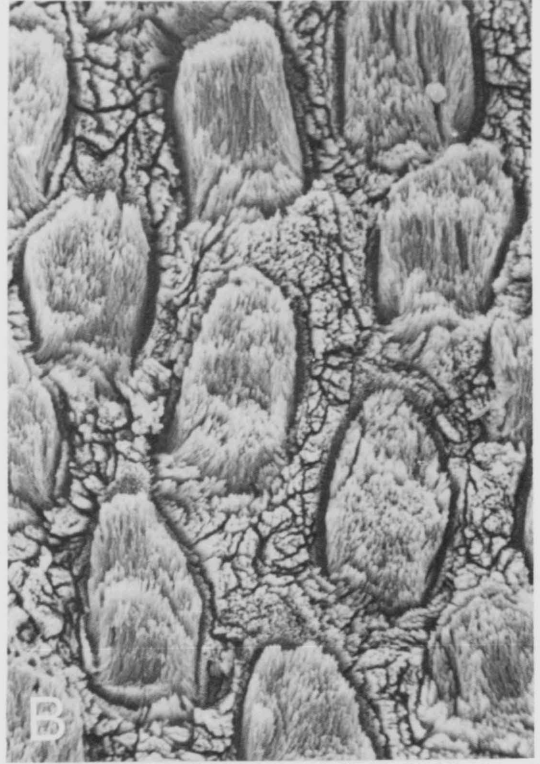


FIG. 7— Variation in depth and orientation of prepared enamel surface. Cross-sections of (A) *Ptilodus* new species A I<sub>1</sub> (700X) and (B) *Taeniolabis taöensis* I<sub>1</sub> (250X) showing positions of ground and etched tangential surfaces examined at designated depths in the enamel. N = number of prisms measured;  $\bar{X}$  = mean prism diameter in  $\mu\text{m}$ ; sd = standard deviation from mean; D = distance from surface of tooth to section, in mm; scale bars = 20  $\mu\text{m}$ . ANOVA results for *Ptilodus*:  $F = 6.53$ ;  $F_{(1,95)}(2,60) = 3.15$ . ANOVA results for *Taeniolabis*:  $F = 3.09$ ;  $F_{(1,95)}(3,48) = 2.80$ . The tangential sections of the *Taeniolabis taöensis* I<sub>1</sub> are illustrated in Figure 8, as indicated.

Cross sections of a *Ptilodus* incisor reveal an abrupt change in prism orientation approximately mid-way through the enamel (Figures 2D and 7A). *Taeniolabis* incisor prisms do not exhibit this change in orientation. Too few cross-sections and longitudinal sections have been examined across a range of taxa to determine whether this change in orientation is characteristic of ptilodontoids as a group. Such an investigation might shed light on the different functional roles envisaged for taeniolabidoid and ptilodontoid incisors (Kielan-Jaworowska, 1980).

FIG. 8— Four tangential sections at successively greater depths in the enamel of *Taeniolabis taöensis* I<sub>1</sub> (all at 1600X; scale bar = 10  $\mu$ m). Position of sections designated in Figure 7B; depths determined from camera lucida drawings of cross-sections of enamel at four stages in the grinding process. Note the similarity of prism size, shape, and density in all four sections.





*Variation within a single individual.*—Potential variability in enamel ultrastructural patterns between incisors, premolars, and molars within a single multituberculate individual has never been investigated directly. A mandible of *Kryptobaatar dashzevegi* containing I<sub>1</sub>, P<sub>4</sub>, M<sub>1</sub>, and M<sub>2</sub> enabled us to examine intra-individual variation in ultrastructure. The pattern in P<sub>4</sub>, M<sub>1</sub>, and M<sub>2</sub> is illustrated in Figure 9. Unfortunately, two attempts to prepare the incisor failed to reveal enamel ultrastructure and we did not want to risk further damage to the specimen. The two molars appear to have more enamel tubules and have shorter and wider prisms than the premolar, but these minor differences may be due to depth and angle of section within the enamel. Based on the single individual studied here, there appears to be a progressive increase in size of prisms posteriorly in the jaw of *Kryptobaatar* (Figure 10). It is inappropriate, however, to generalize from a trend apparent in one individual without direct information on intra-individual variation in other multituberculates.

*Variation within a single species.*—Previous studies have assumed, implicitly, that variation in ultrastructure within one tooth, one individual, and one species is insignificant. With the exception of Sahní (1979), who examined 46 isolated teeth of *Mesodma thompsoni* and *Mesodma formosa*, no study has systematically tested these assumptions. We examined teeth from more than one individual in 19 of the 36 species in this study as an independent check of intraspecific variation. In no case, however, were more than three individuals per species represented. The results of this investigation are presented in Figure 10. Prism shape, circular or arcade, is consistent within individuals of the same species (Figures 11-18). Although prism diameter in conspecific individuals varies by up to 3.0  $\mu\text{m}$  in our sample (e.g., *Eucosmodon primus*, a taeniolabidoid), the average variability is much less (1.2  $\mu\text{m}$ ). Despite this seemingly high variability in prism diameter, our sample sizes per species are too small to be useful statistically. Variation in other, minor, ultrastructural characteristics exists (see figure captions, Figures 11-18, for specific descriptions), but cannot be directly attributed to intraspecific differences.

*Variation within a genus.*—We examined four species of *Ptilodus* (*P.* new species A, *P.* new species B, *P. isosiensis*, and *P. wyomingensis*) and two species of *Microcosmodon* (*M. conus* and *M. rosei*) to compare the enamel ultrastructure between congeneric species. In the species of *Ptilodus*, small, circular prisms are consistently present; in both species of *Microcosmodon*, small, circular and arcade-shaped prisms are present. The variation in prism size among congeneric species appears to be no greater than the average for intraspecific variation (1.2  $\mu\text{m}$ ) (Figure 10). We conclude that major differences (in prism size and shape) are not apparent at this level, although various minor differences do appear. This result is significant in that the principal characters of interest, size and shape of prisms, in single species appear to be representative of the genus as a whole.

*Variation between genera.*—Consistent differences in enamel ultrastructure first appear in the taxonomic hierarchy in comparing multituberculate genera to one another (Figure 10). As mentioned previously, two major ultrastructural patterns are prevalent: large, arcade-shaped prisms and small, circular prisms (Figures 11-18). All but one genus (*Microcosmodon*) fall clearly into one of these two patterns (Figure 19A).

Sahní's (1979:42,46) statements that "isolated teeth of genera can be identified on the basis of ultrastructural studies" and "the major drawback at present for distinguishing taxa at the generic or specific level is the lack of comparative SEM data from diverse phyletic lineages," appear more optimistic than is warranted, considering the results of this study. Two isolated teeth, each exhibiting a different pattern, may be confidently placed in two genera, but two isolated teeth

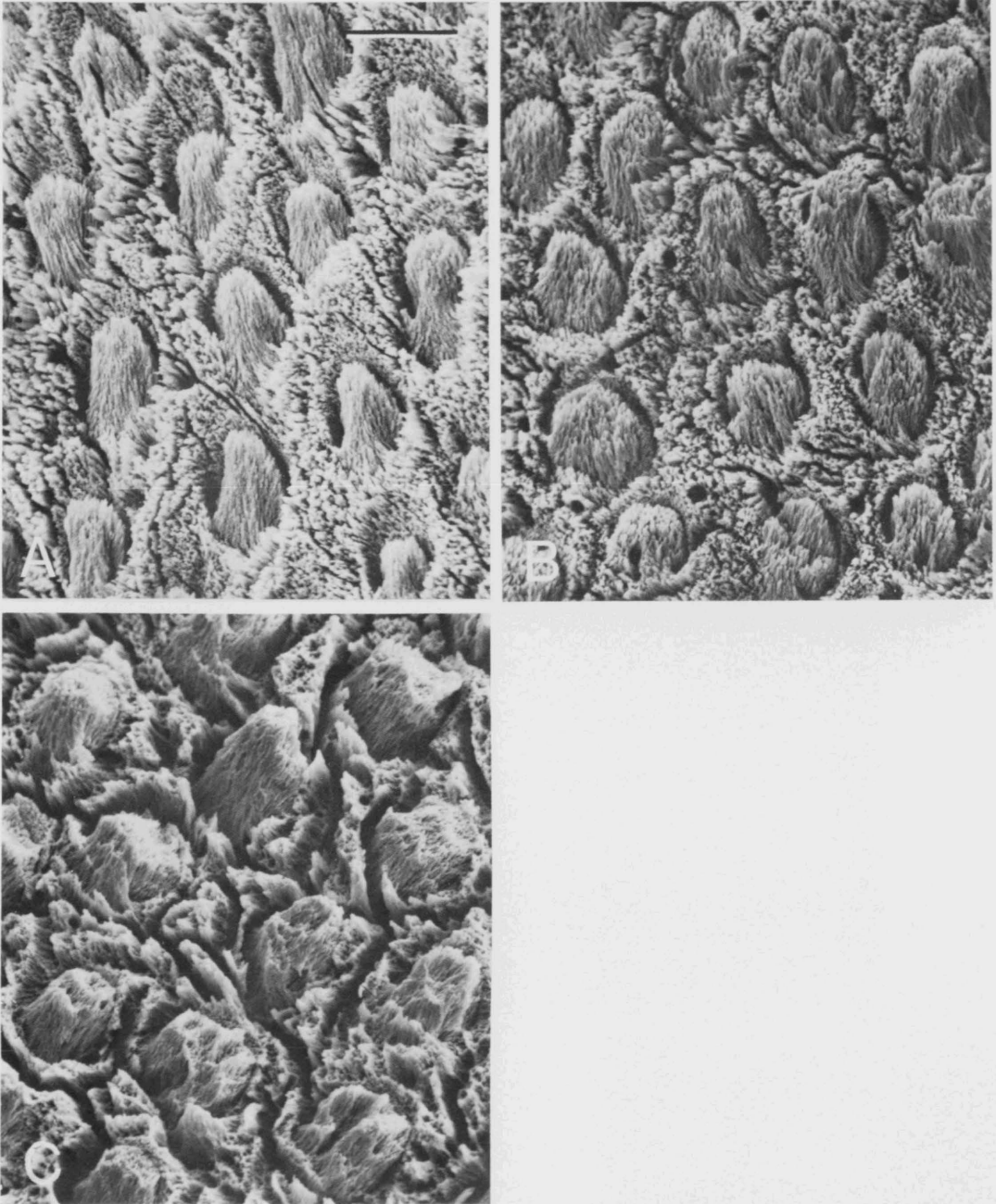


FIG. 9— Variation within a single individual. *Kryptobaatar dashzevegi* P<sub>4</sub> (A), M<sub>1</sub> (B), and M<sub>2</sub> (C), all at 1600X; scale bar = 10  $\mu$ m. Although all three teeth exhibit large, arcade-shaped prisms, P<sub>4</sub> and M<sub>1</sub> are much more similar to one another than either is to M<sub>2</sub>.

FIG. 10— Characteristics of enamel ultrastructure measured and/or calculated from 64 teeth assigned to 32 genera of Late Cretaceous and early Tertiary multituberculates. Average prism diameter per species (measured from photomicrographs) is plotted as a square; solid squares represent circular prisms, open squares represent arcade-shaped prisms, diagonally-filled square represents both circular and arcade-shaped prisms in one genus (*Microcosmodon*), vertical lines denote mean ( $\bar{X}$ ) values, horizontal lines denote one standard deviation (sd) about the mean. N = number of prisms measured per specimen; minimum cross-sectional area =  $(\bar{X})^2$ ; center to center distance is measured from photomicrographs; number of prisms per  $\text{mm}^2 = (2 \times 10^6)/(d^2)(3^{1/2})$ ; interprism area per  $\text{mm}^2 = 1 - (\text{no. prisms per mm}^2)(\text{min. x-sect. area per prism})$ .

SUB-ORDER	FAMILY	SPECIES	PRISM SIZE (µm)											TOOTH POSITION	N	X PRISM DIA	s d	MIN X-SECT AREA	CTR-CTR DISTANCE	NUMBER PRISMS PER mm <sup>2</sup>	INTERPRISM AREA PER mm <sup>2</sup>		
			2	3	4	5	6	7	8	9	10	11	12									13	
PTILODONTIDAE	PTILODONTIDAE	<i>Kimbelohia campi</i>			•										P <sub>4</sub>	25	3.9	0.5	15	7.5	20,500	0.693	
					•										P <sub>4</sub>	17	4.5	0.6	20	8.5	16,000	0.680	
		<i>Prochetodon cavus</i>	•													P <sub>4</sub>	22	2.6	0.4	7	5.1	44,400	0.689
					•											M <sup>1</sup>	25	3.7	0.6	14	7.0	23,600	0.670
		<i>Ptilodus isosiensis</i>			•											P <sub>4</sub>	19	3.8	0.6	14	7.4	21,100	0.705
		<i>Ptilodus wyomingensis</i>			•											I <sub>1</sub>	20	4.7	0.3	22	8.6	15,600	0.657
					•											P <sub>4</sub>	23	3.5	0.4	12	8.0	18,000	0.784
					•											M <sub>1</sub>	22	3.2	0.6	10	5.7	35,500	0.646
		<i>Ptilodus new species A</i>			•											P <sub>4</sub>	62	2.8	0.5	8	7.1	22,900	0.817
		<i>Ptilodus new species B</i>			•											I <sub>1</sub>	23	4.8	0.6	23	10.8	9,900	0.772
				•											P <sub>4</sub>	22	3.5	0.7	12	8.6	15,600	0.813	
				•											M <sup>1</sup>	38	3.7	0.7	14	9.1	13,900	0.805	
	NEOPLAGIOLAICIDAE	<i>Ectypodus powelli</i>			•										I <sub>1</sub>	12	3.8	0.4	14	8.7	15,300	0.786	
					•										P <sub>4</sub>	20	2.9	0.4	8	8.8	14,900	0.881	
					•										M <sup>1</sup>	19	3.0	0.8	9	8.6	15,600	0.860	
		<i>Mesodma sp.</i>			•										P <sub>4</sub>	32	3.6	0.7	13	7.9	18,500	0.760	
		<i>Mimelodon silberlingi</i>			•										P <sub>4</sub>	31	3.1	0.4	10	7.6	20,000	0.800	
					•										M <sub>1</sub>	27	3.1	0.4	10	7.4	21,100	0.789	
		<i>Neoplagiulaox hunteri</i>			•										P <sub>4</sub>	58	3.2	0.5	10	6.5	27,300	0.727	
		<i>Pareclypodus lunatus</i>			•										I <sub>1</sub>	65	2.7	0.4	7	7.3	21,700	0.848	
				•										P <sub>4</sub>	34	2.7	0.4	7	6.6	26,500	0.815		
	<i>Xanclomys mcgrewi</i>			•										P <sub>4</sub>	20	1.9	0.4	4	5.9	33,200	0.867		
	CIMOLODONTIDAE	<i>Anconodon russelli</i>			•										P <sub>4</sub>	28	3.4	0.4	12	7.1	22,900	0.725	
		<i>Liotomus marshi</i>			•										P <sub>4</sub>	55	3.5	0.5	12	8.0	18,000	0.784	
		<i>Cimolodon nitidus</i>								□					P <sub>4</sub>	24	8.0	0.8	64	15.7	4,700	0.699	
									□					M <sub>1</sub>	40	7.0	0.6	49	11.7	8,400	0.588		
BOFFI-DAE	<i>Boffius splendidus</i>													M	8	11.8	1.7	139	24.1	2,000	0.722		
TAENIOLABIDOIDEAE	TAENIOLABIDAE	<i>Taeniolabis taoensis</i>													I <sub>1</sub>	63	10.1	1.4	102	20.8	2,700	0.725	
															P <sub>4</sub>	20	8.3	0.9	69	16.0	4,500	0.690	
															M <sub>2</sub>	23	10.2	1.6	104	23.7	2,100	0.732	
		<i>Catopsalis joyneri</i>													I <sub>2</sub>	18	9.8	1.7	95	19.0	3,200	0.693	
															P <sub>4</sub>	30	8.1	1.0	66	16.5	4,200	0.723	
															M <sub>1</sub>	25	7.5	0.7	56	15.7	4,700	0.737	
		<i>Prionessus lucifer</i>													M <sub>2</sub>	29	8.4	0.9	71	15.7	4,700	0.666	
		<i>Sphenopsalis nobilis</i>													M <sub>2</sub>	33	7.1	0.6	50	13.0	6,800	0.660	
		<i>Lambdopsalis bulla</i>													M <sub>2</sub>	30	7.7	0.5	59	15.9	4,600	0.729	
		EUCOSMODONTIDAE	<i>Eucosmodon primus</i>													I <sub>1</sub>	22	9.9	1.2	98	17.9	3,600	0.647
															P <sub>4</sub>	41	6.9	0.7	48	13.2	6,600	0.683	
	<i>Slygimys kuszmauli</i>														I <sub>2</sub>	13	7.9	0.4	62	14.3	5,600	0.653	
															P <sub>4</sub>	29	9.3	1.2	86	17.8	3,600	0.690	
															M <sub>1</sub>	22	9.4	0.9	88	16.1	4,500	0.604	
	<i>Neoliotomus ultimus</i>														I <sub>1</sub>	22	5.3	1.0	28	10.0	11,500	0.678	
															P <sub>4</sub>	45	4.0	0.7	16	8.4	16,400	0.738	
															M <sup>1</sup>	15	4.6	1.4	21	8.5	16,000	0.664	
	<i>Xyronomys sp.</i>														P <sub>4</sub>	36	4.2	0.5	18	8.0	18,000	0.676	
	<i>Kryptobaatar dashzevegi</i>														P <sub>4</sub>	18	6.0	0.8	36	13.6	6,200	0.777	
															M <sub>1</sub>	18	7.3	0.9	53	13.4	6,400	0.661	
														M <sub>2</sub>	13	8.3	1.3	69	14.9	5,200	0.641		
<i>Microcosmodon conus</i>													P <sub>4</sub>	54	5.4	0.7	29	10.5	10,500	0.696			
<i>Microcosmodon rosei</i>													I <sub>2</sub>	28	4.3	0.7	18	10.8	9,900	0.822			
													M <sub>1</sub>	21	4.7	0.4	22	10.0	11,500	0.747			
<i>Pentacosmodon pronus</i>													P <sub>4</sub>	16	8.3	0.9	69	11.6	8,600	0.407			
													M <sub>1</sub>	22	6.8	0.8	46	11.9	8,200	0.623			
INCERTAE SEDIS	CIMOLOMYIDAE	<i>Cimolomys clarki</i>												P <sub>4</sub>	13	8.5	0.8	72	14.7	5,300	0.618		
														M <sub>1</sub>	18	8.5	0.5	72	14.2	5,700	0.590		
		<i>Meniscoaessus robustus</i>												I <sub>2</sub>	17	8.6	0.9	74	15.6	4,700	0.652		
														P <sub>4</sub>	11	9.8	1.0	96	17.8	3,600	0.654		
														M <sub>2</sub>	10	9.5	0.9	90	22.8	2,200	0.802		
	<i>Essonodon browni</i>													M <sub>1</sub>	38	8.1	0.9	66	12.4	7,500	0.505		
	INCERTAE SEDIS	<i>Cimexomys minor</i>												P <sub>4</sub>	27	6.9	0.7	48	12.9	6,900	0.669		
														M <sup>1</sup>	37	6.3	1.1	40	10.8	9,900	0.604		
		<i>Paracimexomys magister</i>												M <sup>1</sup>	44	6.1	1.2	37	11.1	9,400	0.652		
		<i>Hainina belgica</i>												M <sup>1</sup>	35	6.9	0.7	48	15.8	4,600	0.779		
<i>Viridomys orbatus</i>													P <sub>4</sub>	?	?	?	?	?	?	?			

FIG. 11— Representative photomicrographs of ptilodontoid multituberculates (1600X; scale bar = 10  $\mu\text{m}$ ). (A) *Kimbetohia*. Prismatic structure relatively poorly revealed; poor to fair prism sheath development; no enamel tubules. (B) *Prochetodon*. Prisms well-defined; good sheath development; no enamel tubules. (C) *Ptilodus*. Prisms fairly well-defined; fair sheath development; few or no enamel tubules. (D) *Ectypodus*. Fusiform to circular prisms arranged in sinuous columns; good sheath development; no enamel tubules.

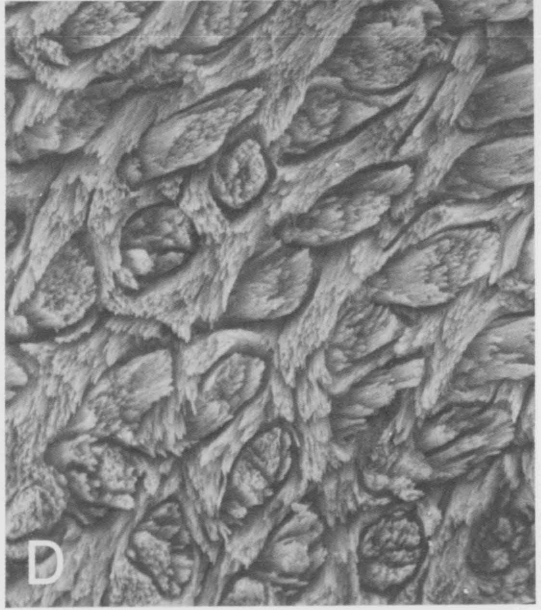
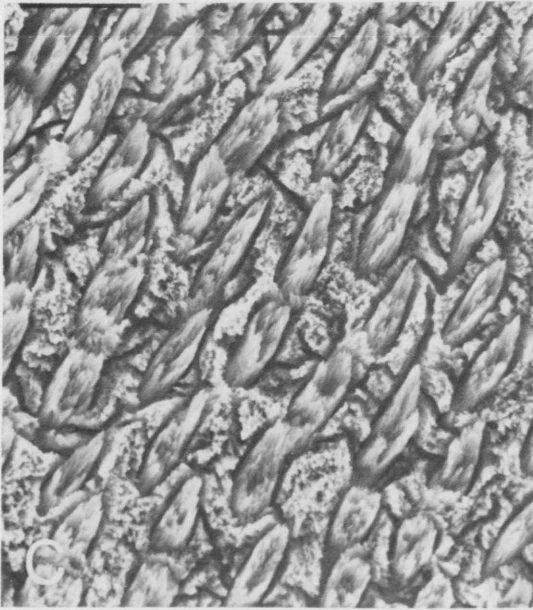


FIG. 12— Representative photomicrographs of ptilodontoid multituberculates (1600X; scale bar = 10  $\mu\text{m}$ ). (A) *Mesodma*. Prisms fairly well-defined; occasionally exhibits small, arcade-shaped prisms near the enamel-dentine junction; fair sheath development; no enamel tubules. (B) *Mimetodon*. Prisms well-defined; fair to good sheath development; few to no enamel tubules. (C) *Neoplagiaulax*. Prisms well-defined; fair to good sheath development; few enamel tubules. (D) *Parecypodus*. Prismatic structure well-defined; good sheath development; few enamel tubules.



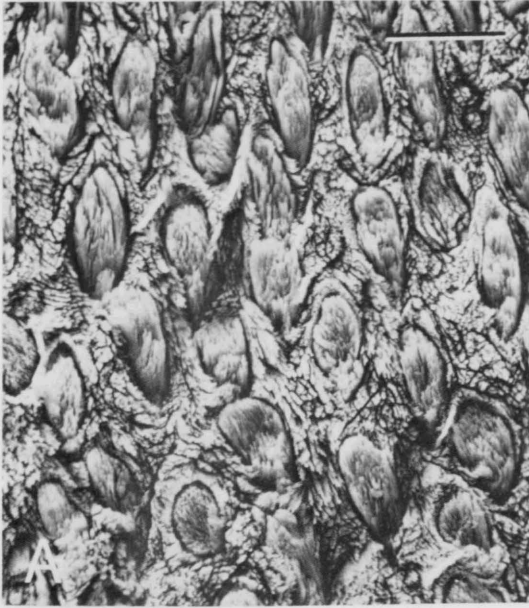


FIG. 13— Representative photomicrographs of ptilodontoid multituberculates (1600X; scale bar = 10  $\mu\text{m}$ ). (A) *Xanclomys*. Prisms fairly well-defined; smallest prisms measured in this study; good sheath development; few to several enamel tubules. (B) *Anconodon*. Prisms well-defined; moderately good sheath development; no enamel tubules. (C) *Liotomus*. Prisms fairly well-defined; fair sheath development; few to no enamel tubules. (D) *Cimolodon*. Prisms fairly well-defined, slightly wider than long; unusual for ptilodontoids in possessing large, arcade-shaped prisms; fair sheath development; unusual diagenetic (?) fabric in one tooth examined; no enamel tubules.

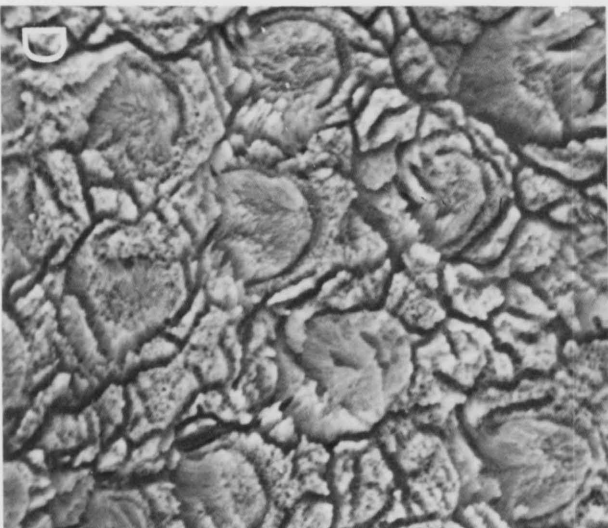
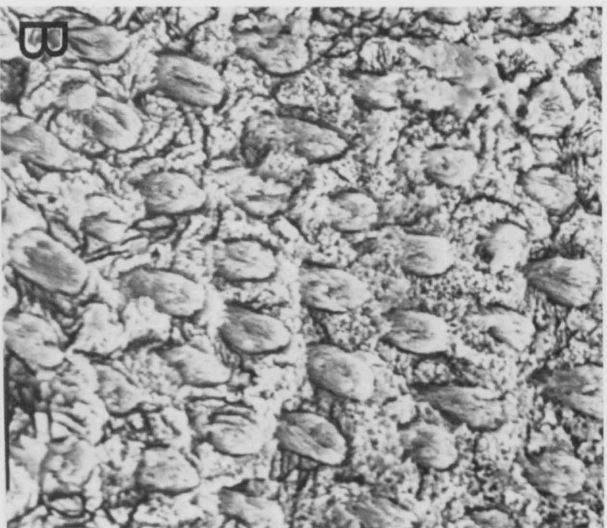
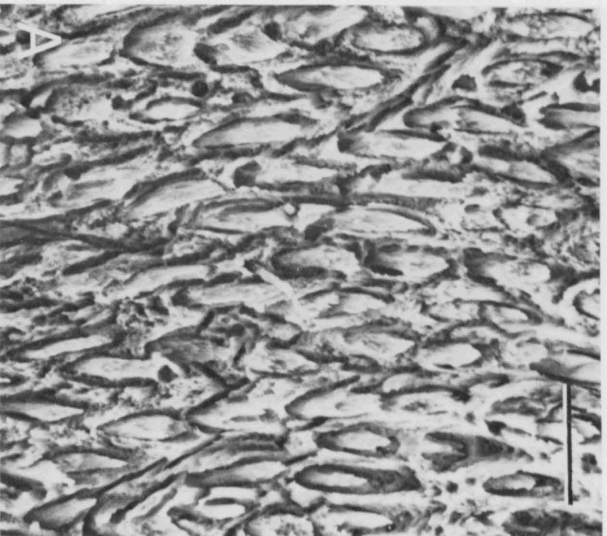


FIG. 14— Representative photomicrographs of ptilodontoid and taeniolabidoid multituberculates (1600X; scale bar = 10  $\mu\text{m}$ ). (A) *Boffius*. Prisms relatively poorly defined; largest and most widely spaced prisms measured in this study; unusual for ptilodontoids in possessing large, arcade-shaped prisms; poor to fair sheath development; few to no enamel tubules. (B) *Taeniolabis*. Prisms very well-defined, regularly arranged; sheaths well-developed; few enamel tubules. (C) *Catopsalis*. Prisms well-defined, regularly arranged; sheaths well-developed; few to no enamel tubules. (D) *Prionessus*. Prisms relatively poorly defined; sheaths poorly developed; no enamel tubules.

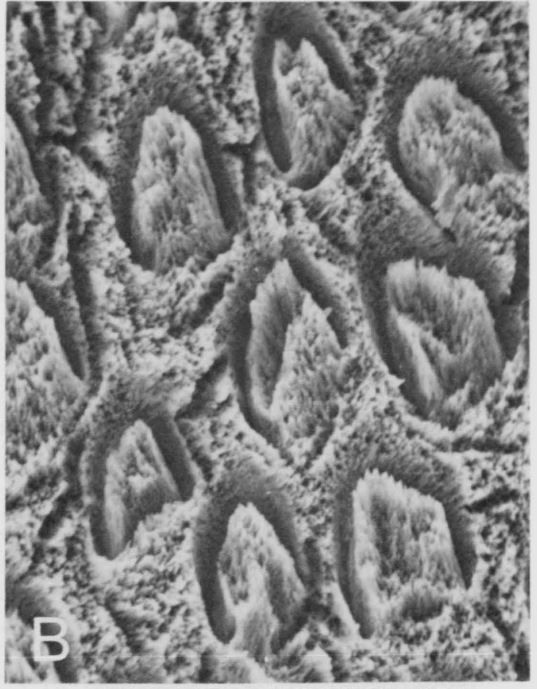
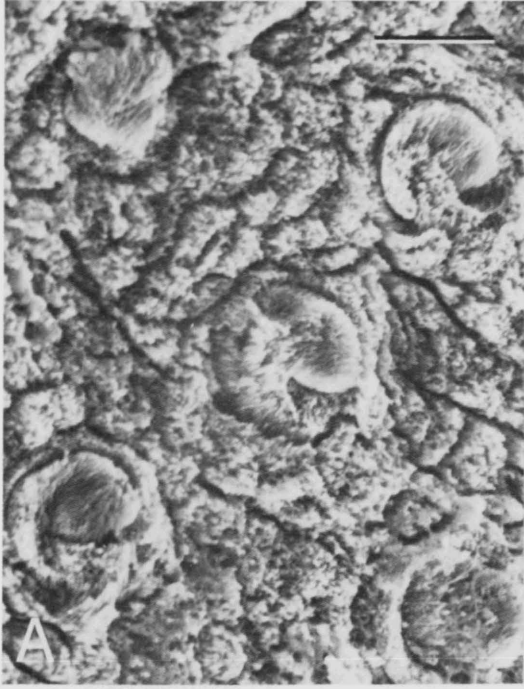


FIG. 15— Representative photomicrographs of taeniolabidoid multituberculates (1600X; scale bar = 10  $\mu\text{m}$ ). (A) *Sphenopsalis*. Prisms well-defined, very regularly arranged; sheaths well-developed, often meeting under prism, forming a flat “base;” few enamel tubules. (B) *Lambdopsalis*. Prisms well-defined, regularly arranged; sheaths well-developed, also occasionally forming a “base” under prisms; few to no enamel tubules. (C) *Eucosmodon*. Prisms well-defined, often wider than long, very regularly arranged; sheaths relatively well-developed; no enamel tubules. (D) *Stygimys*. Prisms relatively well-defined, fairly regularly arranged; fair sheath development; few to no enamel tubules.



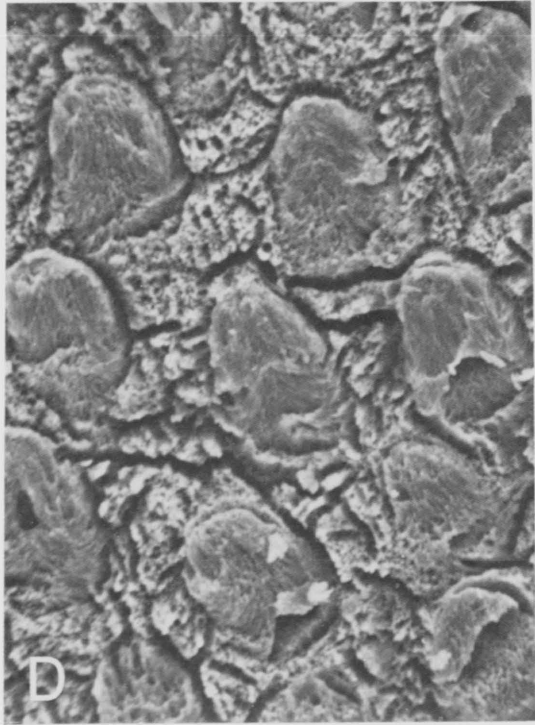
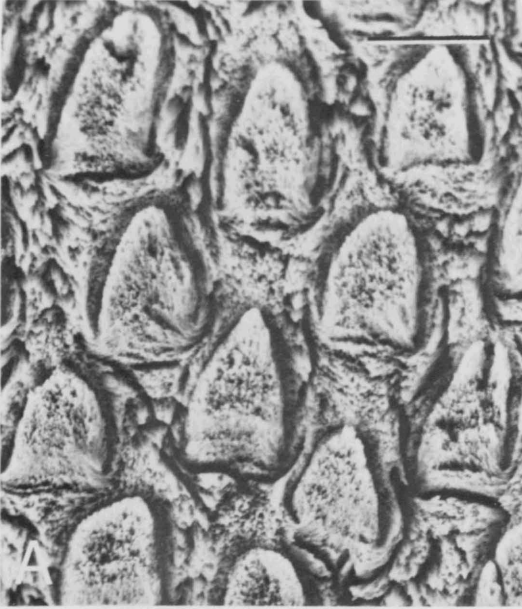


FIG. 16— Representative photomicrographs of taeniolabidoid multituberculates (1600X; scale bar = 10  $\mu\text{m}$ ). (A) *Neoliotomus*. Prisms well-defined, often in fairly well-defined, sinuous columns; round to somewhat fusiform prisms; unusual for taeniolabidoids in possessing small, circular prisms; sheaths well-developed; no enamel tubules. (B) *Xyronomys*. Prisms relatively well-defined; unusual for taeniolabidoids in possessing small, circular prisms; sheaths well-developed; no enamel tubules. (C) *Kryptobaatar*. Prisms well-defined, fairly regularly arranged, occasionally wider than long; well-developed sheaths; several enamel tubules. (D) *Microcosmodon*. Prisms well-defined, fairly regularly arranged; note both circular and arcade-shaped prisms adjacent to one another; sheaths well-developed; several enamel tubules.



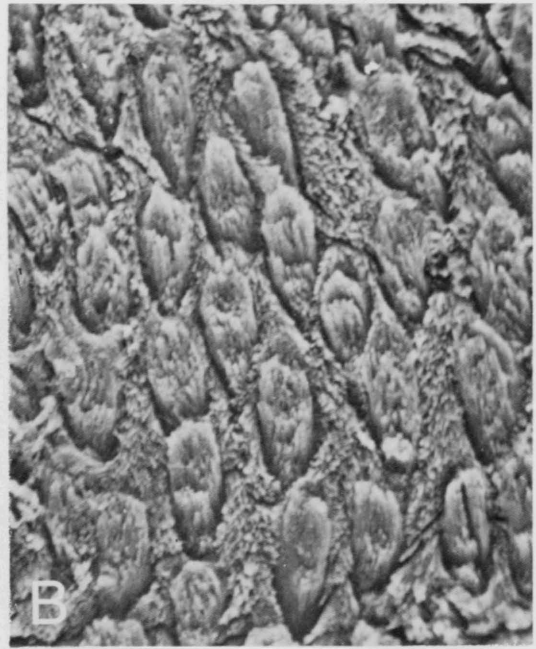
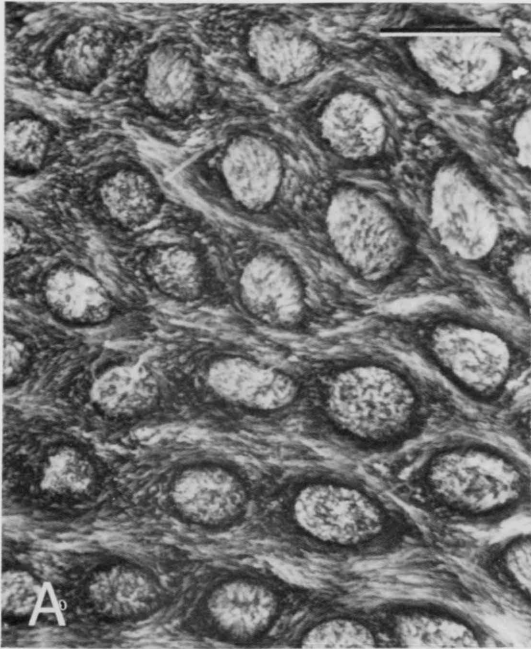


FIG. 17— Representative photomicrographs of taeniolabidoid multituberculates and genera whose subordinal assignment is uncertain (1600X; scale bar = 10  $\mu\text{m}$ ). (A) *Pentacosmodon*. Prisms poorly defined; fairly poorly developed sheaths; few enamel tubules. (B) *Cimolomys*. Prisms moderately well-defined; sheaths fairly well-developed; few to no enamel tubules. (C) *Meniscoessus*. Prisms very well-defined, regularly arranged; well-developed sheaths; several to many enamel tubules. (D) *Essonodon*. Prisms fairly well-defined; sheaths fairly well-developed; several enamel tubules.

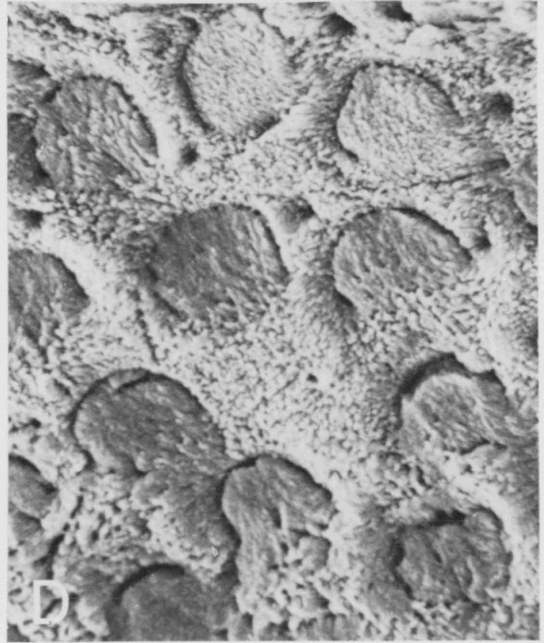
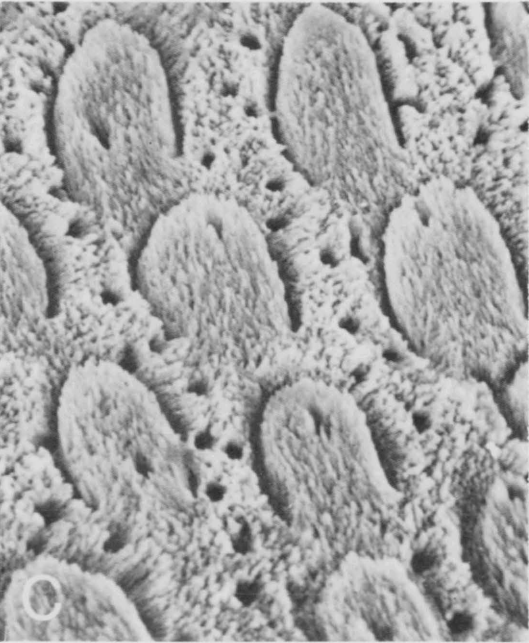
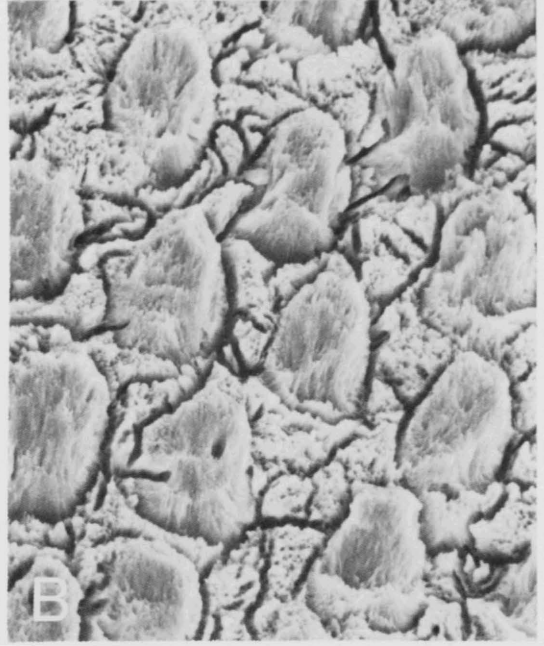
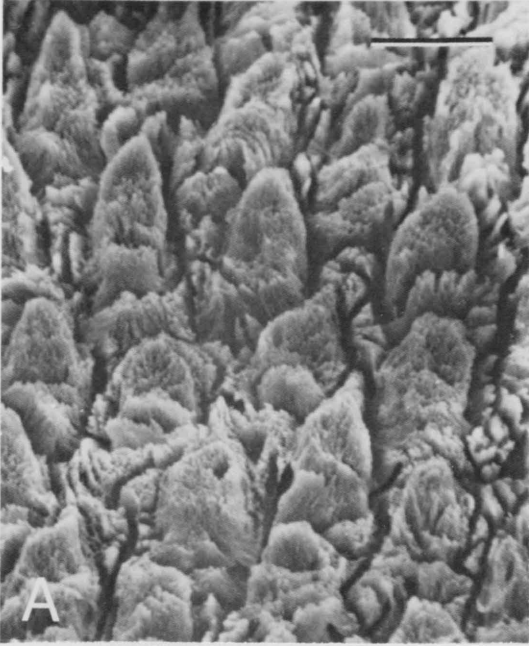
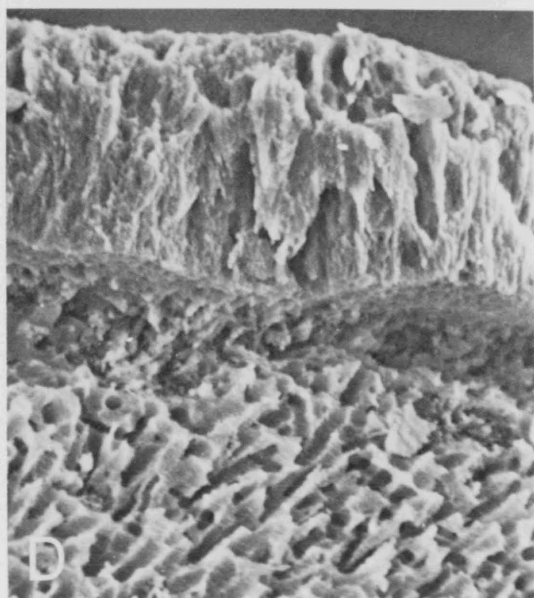
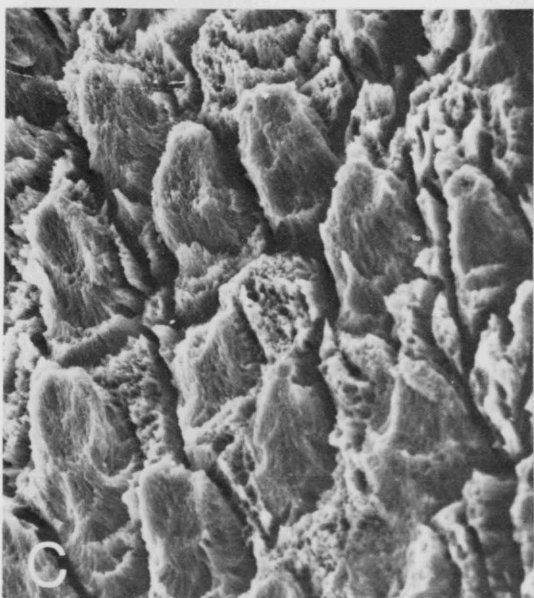
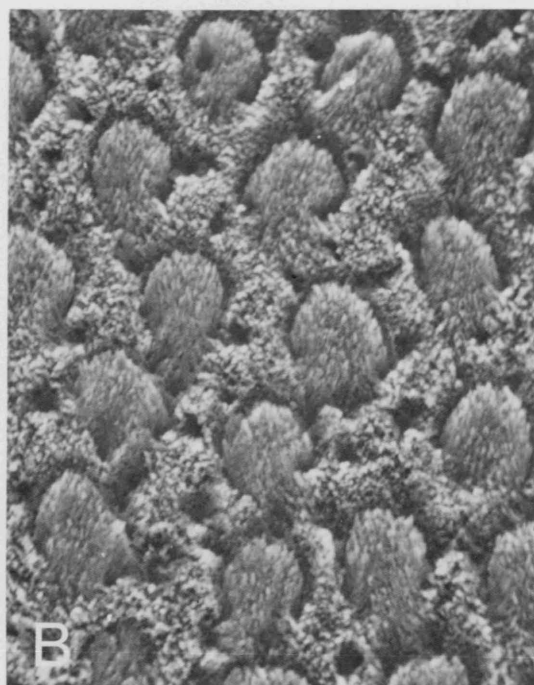
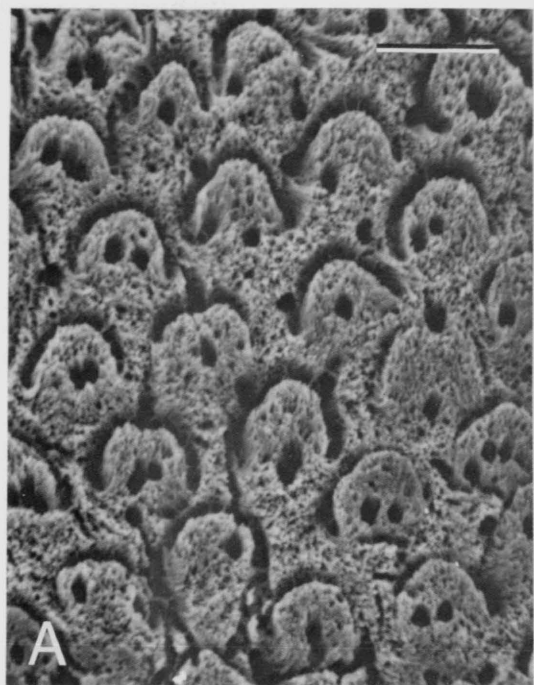


FIG. 18— Representative photomicrographs of multituberculates whose subordinal assignment is uncertain (1600X; scale bar = 10  $\mu\text{m}$ ). (A) *Cimexomys*. Prisms well-defined, fairly regularly arranged, occasionally bilobed; well-developed sheaths; many enamel tubules. (B) *Paracimexomys*. Prisms relatively well-defined; sheaths well-developed; several to many enamel tubules. (C) *Hainina*. Prisms poorly defined; sheaths poorly developed; no enamel tubules. (D) *Viridomys*. No divergence of crystallites apparent. Enamel appears to be nonprismatic.



with prisms of the same general size and shape may belong to either the same genus or to two different genera. Nevertheless, a variety of additional features observable in Figures 11-18 do serve to distinguish certain genera from others. *Eucosmodon* and *Sphenopsalis* exhibit prisms arranged in an unusually regular two-dimensional array. *Sphenopsalis* has arcade-shaped prisms, but prism sheaths often extend across the "base" of the arcade, isolating prismatic from interprismatic crystallites. *Ectypodus* has fusiform prisms arranged in sinuous columns. *Cimexomys* and *Kryptobaatar* have arcade-shaped prisms that occasionally appear bilobed. *Cimexomys* and *Paracimexomys* are the only genera with relatively abundant enamel tubules. *Microcosmodon*, *Kryptobaatar*, and *Essonodon* exhibit some tubules; all other genera appear to be devoid of tubules.

*Microcosmodon* is perhaps the most distinctive of all genera examined. Its teeth are consistently different in possessing both circular and arcade-shaped prisms adjacent to one another (Figure 16D). Few cases have been reported where more than one prism shape is present in the same species. The most significant exceptions are in the great apes and some Old World monkeys (Boyde and Martin, 1982, 1984), where both arcade-shaped and circular prisms can occur in the same section. In these taxa, as in our sample of *Microcosmodon*, arcade-shaped prisms predominate over circular ones. The only other genus giving evidence of more than one prism shape is *Mesodma*. Although Sahni (1979) reported only circular prisms in *Mesodma*, one of our sections exhibits both circular and arcade-shaped prisms. This section, however, is adjacent to the enamel-dentine junction and is therefore much deeper than most other sections examined. As Boyde and Martin (1982, 1984) showed for several higher primates, it is not unusual to obtain circular prisms near the enamel-dentine junction in taxa that otherwise have arcade-shaped prisms. This explanation apparently cannot be used to account for the presence of two prism shapes in *Microcosmodon*, because both circular and arcade-shaped prisms were revealed in all sections of *Microcosmodon*, despite the level examined.

Our investigation reveals only large, arcade-shaped prisms in *Stygimys*, in contrast to the results of Sahni (1979) and Fosse et al. (1978). Sahni (1979:45) concluded that *Stygimys* has open, horseshoe-shaped prisms, but that prisms "in sections viewed normal to long axes are round." Fosse et al. (1978:57) stated that, with the exception of *Stygimys*, in all multituberculates examined, "the prisms are arcade-shaped as normally found in mammalian enamel." They note, however, that "arcade-shaped prisms were found in other enamel areas of *Stygimys kuszmauli*" (Fosse et al., 1978:60). Sahni (1979) noted that *Stygimys* possessed the largest enamel prisms of all the multituberculates he studied. Our larger sample reveals that several genera (*Catopsalis*, *Taeniolabis*, *Eucosmodon*, *Meniscoessus*, and particularly *Boffius*) have prism diameters that are larger than the largest observed in *Stygimys*. *Xanclomys* had the smallest prism diameters (1.9  $\mu\text{m}$ ) of all genera examined in this study.

*Variation within suprageneric taxa.*—Most studies of multituberculate enamel ultrastructure have compared differences between the suborders Ptilodontoidea and Taeniolabidoidea. To interpret and compare our results at this level, we provisionally accept Hahn and Hahn's (1983) classification of multituberculates (see Table 1). Our results indicate that there is a strong correlation between prism size and shape and subordinal level in multituberculate tooth enamel (Figure 19 A,B); they generally support the assertion that, among multituberculates, prism diameters of taeniolabidoids are markedly greater than those of ptilodontoids (Fosse et al., 1978; Sahni, 1979). However, not all taeniolabidoids, as currently defined, possess "gigantoprismatic" enamel (Figure 10). Taeniolabidids all have large, arcade-shaped prisms; most eucosmodontid genera also exhibit large, arcade-shaped prisms but some (*Neoliotomus* and *Xyronomys*) possess small, circular prisms; one (*Microcosmodon*) possesses an unusual combination of both.

Among ptilodontoids, all ptilodontids and neoplagiaulacids examined have small, circular prisms. Cimolodontids all have small, circular prisms except for *Cimolodon*, which has large, arcade-shaped prisms. *Boffius*, classified as a monotypic family in the Ptilodontoidea, has exceptionally large, arcade-shaped prisms.

Four of the five genera that do not fit the otherwise consistent association of large, arcade-shaped prisms in taeniolabidoids and small, circular prisms in ptilodontoids are problematic in other aspects of their morphology as well. The taxonomic position of *Neoliotomus* has been questioned previously (Krause, 1982a) and both *Xyromys* and *Boffius* are known only from a few isolated teeth; their gross dental morphology does not *clearly* indicate taxonomic affinities with either suborder. Although no one has doubted the affinities of *Microcosmodon* with other undoubted taeniolabidoids, it possesses an ultrastructural pattern that unambiguously aligns it with neither the Ptilodontoidea nor the Taeniolabidoidea. Similarly, no one has questioned that *Cimolodon* is an undoubted ptilodontoid but, inexplicably, *Cimolodon* exhibits the large, arcade-shaped prisms typical of taeniolabidoids.

With the exception of *Viridomys*, all genera currently placed in Suborder *incertae sedis* exhibit large, arcade-shaped prisms. These genera include *Cimolomys*, *Meniscoessus*, *Essonodon*, *Cimexomys*, *Paracimexomys*, and *Hainina*. *Viridomys* appears to be unique among Late Cretaceous and early Tertiary multituberculates in lacking prisms. We must qualify our assessment however by noting that only one small area on one tooth was prepared for examination. *Viridomys* is known from only two isolated teeth; we are reluctant to risk any further damage to the available material to investigate this apparently unusual ultrastructure.

In addition to prism size and shape, several other parameters reveal a bimodal distribution that generally corresponds with the suborders Ptilodontoidea and Taeniolabidoidea. Most ptilodontoids have many, closely-spaced prisms per unit area and taeniolabidoids have relatively few, widely-spaced prisms per unit area (Figure 19 C,D). Again, *Xyromys* and *Neoliotomus* tend to group with the ptilodontoids while *Cimolodon*, *Boffius*, and the genera currently classified as Suborder *incertae sedis* group with the taeniolabidoids. The bimodality is less clear when comparing the amount of interprismatic material in the two suborders although, in general, ptilodontoids have more interprismatic material than do most taeniolabidoids (Figure 19E).

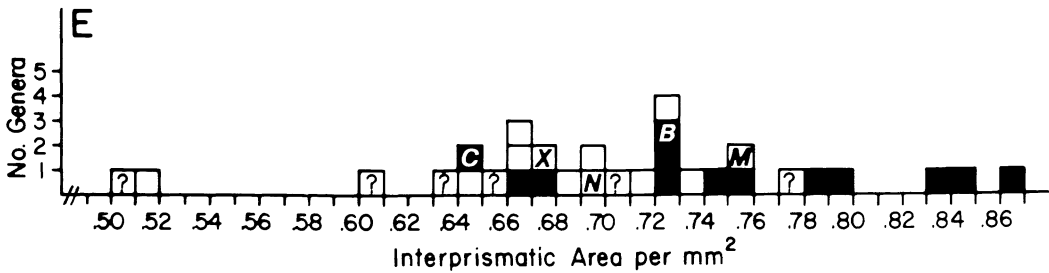
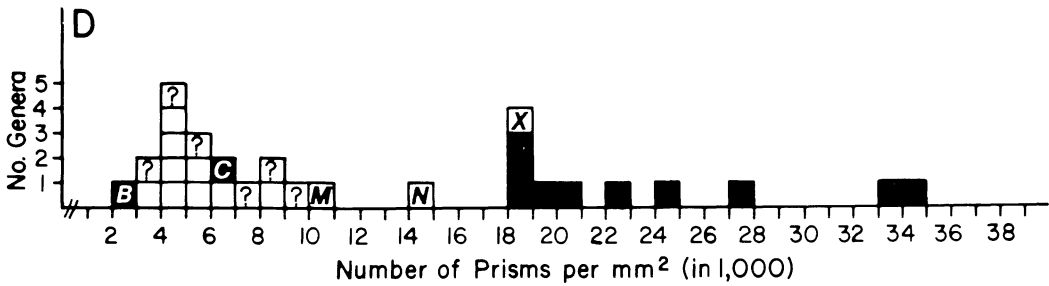
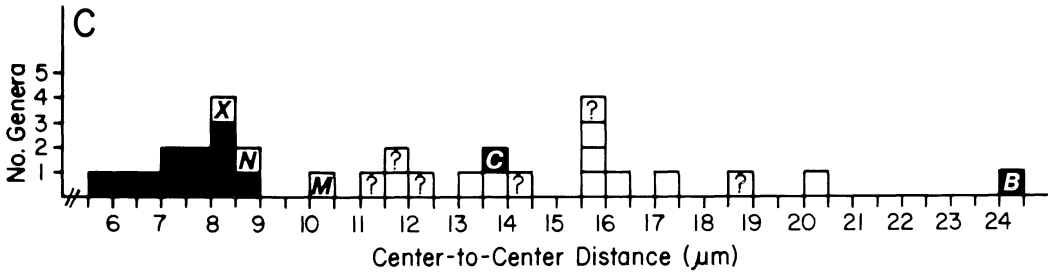
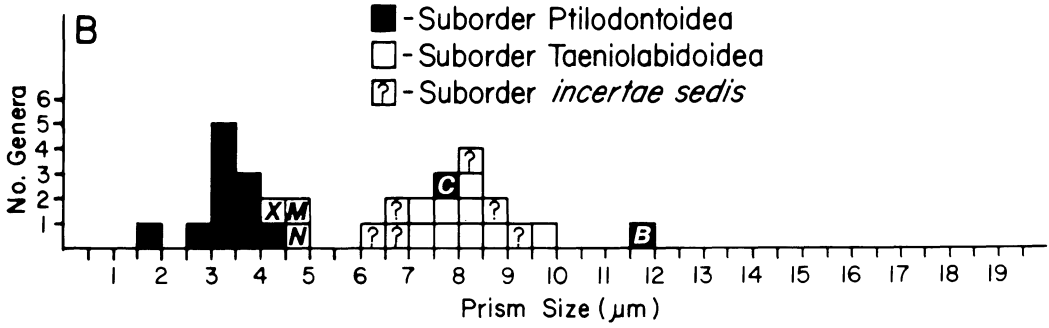
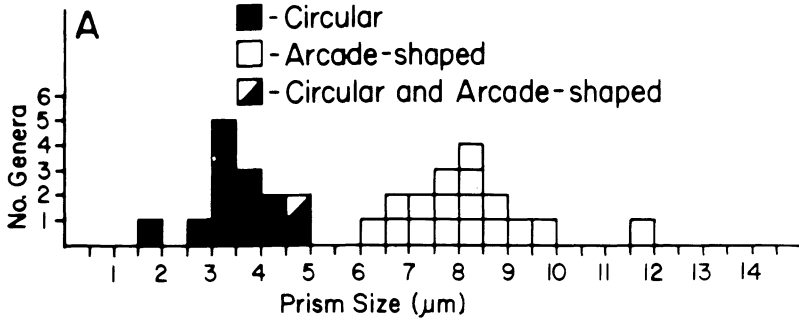
Only five of the 25 genera included in our sample, currently assigned to either the Ptilodontoidea or Taeniolabidoidea, do not possess the ultrastructure predicted on the basis of their subordinal assignment. Of these five, the subordinal affinities of only one (*Cimolodon*) have not been questioned previously. What are the taxonomic implications of these results? In retaining the established suprageneric classification we would conclude that ultrastructure is sometimes, but not always, diagnostic of phylogenetic affinity. If it could be argued that large, arcade-shaped prisms are homologous in all multituberculates in which they occur, and that they represent a derived condition with respect to small, circular prisms, this character could potentially be used to redefine the suborder Taeniolabidoidea.

#### TAENIOLABIDOID MONOPHYLY

The status of the Taeniolabidoidea as a "natural" or monophyletic group has been a central issue in recent discussions of the higher-level phylogeny of the Multituberculata (Clemens and Kielan-Jaworowska, 1979; Kielan-Jaworowska, 1974, 1980; Krause, 1982a). This suborder was originally defined by Sloan and Van Valen (1965:222) as: "including multituberculates in which the enamel of the lower incisor is restricted to the ventro-lateral surface of the tooth, producing a

Fig. 19— (A) Frequency distribution of prism size and shape. The distribution is clearly bimodal; circular prisms are small and arcade-shaped prisms are large. The single exception is *Microcosmodon*, which has both circular and arcade-shaped prisms. (B-E) Frequency distributions of prism size (B), prism spacing (C), prism density (D), and amount of interprismatic material (E), according to subordinal assignment. Bimodal distributions, particularly evident in (B-D), consist of ptilodontoid genera in one cluster and taeniolabidoid genera and genera of uncertain subordinal assignment in the other. Notable exceptions to this pattern include the following genera: *Boffius* (represented by the letter *B*), *Cimolodon* (*C*), *Microcosmodon* (*M*), *Neoliotomus* (*N*), and *Xyronomys* (*X*). The legend shown in histogram (B) also applies to histograms (C) through (E).





self-sharpening tooth similar to that of rodents.” Because a restricted band of enamel has evolved several times independently in the class Mammalia (in rodents, primates, and tillodonts, for example), it is reasonable to hypothesize that this character state has arisen independently more than once within multituberculates. It has not yet been argued convincingly that a restricted band of enamel is both *homologous* in all multituberculates in which it occurs, and is *derived* with respect to a continuous layer of enamel on the incisor. One approach to investigating taeniolabidoid monophyly is to choose another, presumably independent, character and document its distribution within the suborder, as defined by Sloan and Van Valen (1965). If one can argue that this second character is both homologous and derived, and if its distribution is consistent with the distribution of a restricted enamel band in multituberculates, then the results of such a test will tend to support an hypothesis of monophyly.

Kielan-Jaworowska (1974:29) presented the first direct challenge to the taxonomic status of the suborder Taeniolabidoidea. “In the present paper I accept for the time being Sloan and Van Valen’s (1965) division of the later Multituberculata into the Ptilodontoidea and Taeniolabidoidea. I am not happy with this division as I think that the taeniolabidoid type of the lower incisor arose independently at least twice in multituberculate evolution. The suborder Taeniolabidoidea is thus of polyphyletic (at least diphyletic) origin.”

In a paper devoted primarily to revising the taxonomic position of *Gobibaatar* (now a junior synonym of *Kryptobaatar*), Kielan-Jaworowska (1980:169) indicated that she has since rejected the polyphyly hypothesis. “The differences between the two suborders as defined by Sloan and Van Valen (1965), concerning the structure of the enamel cap on the lower incisor may appear minute, but they are accompanied by other important anatomical and functional features. Taken together they show that the Ptilodontoidea and Taeniolabidoidea are well-defined, very distinct suborders.” According to Kielan-Jaworowska, these “other important anatomical and functional features” include: (1) shape of the lower incisors and accompanying functional scenarios regarding their adaptation for piercing (in the Ptilodontoidea) or gnawing (in the Taeniolabidoidea), and (2) the relative size of P<sub>4</sub> (generally large in ptilodontoids and usually small in taeniolabidoids).

Krause (1982a:291) supported the plausibility of polyphyly in a discussion of the uncertain phylogenetic affinities of *Neoliotomus*. “*Neoliotomus* is ... derived relative to the Late Cretaceous eucosmodontines from Asia and primitive relative to those from North America. It is, however, not intermediate in either a morphological or phylogenetic sense ... .” This observation is at least consistent with the independent origin of a restricted enamel band on the lower incisor in more than one group of multituberculates, yet does not, by itself, constitute a strong case for polyphyly. It may, in fact, be entirely consistent with an hypothesis of monophyly.

While the notion of taeniolabidoid polyphyly has been prominent in the literature during the past ten years, it has not received the thorough investigation it requires. When Fosse et al. (1978) presented the preliminary results of their investigation of enamel ultrastructure, it was tempting to think that a reliable and independent source of data had been revealed by improved microanalytical techniques and that this discovery might resolve the problem of taeniolabidoid monophyly.

Before ultrastructural data are used uncritically to reconstruct phylogenies or reorganize classifications, it is necessary to establish their reliability and demonstrate their usefulness (see Rieger and Tyler, 1979). Having analyzed, in this study, several inclusive levels of variability of enamel ultrastructure in ptilodontoid and taeniolabidoid multituberculates, we have greater confidence to proceed with a careful re-evaluation of the higher-level phylogeny of multituberculates. Such an analysis is an obvious (and quite interesting) utilization of these results, but for logistical reasons cannot be included in the present paper.

Thorough studies of enamel ultrastructure in eutherian and metatherian mammals can yield exciting and enlightening results regarding the taxonomic distribution of ultrastructural types. As more information is gathered, it becomes increasingly likely that ultrastructure will be used to critically test hypotheses of relationship established on the basis of gross morphological characters alone.

### SUMMARY AND CONCLUSIONS

1. Enamel prism size (average diameter), shape (circular or arcade-shaped), spacing, and density are found to be the most consistently useful distinguishing ultrastructural characters in multituberculates. Several other features, such as the nature of prism sheaths, spatial arrangement of prisms, nature and amount of interprismatic material, and the nature of enamel tubules, may be, but are not necessarily, useful at some levels of comparison.

2. Different preparation techniques can reveal qualitative differences in enamel ultrastructure, but not necessarily quantitative differences in average prism diameter and mutual central distances between prisms.

3. Comparing prism size, shape, spacing, and density in 64 teeth assigned to 32 multituberculate genera, variability in enamel ultrastructure was detected at different positions on a single tooth, at different depths in the enamel, within teeth of a single individual and single species, and between different genera. All teeth could be unambiguously assigned to one of two size populations that usually, but not always, corresponded to the two prism shapes encountered in multituberculates.

4. Our results clearly indicate that all multituberculates do not exhibit circular prisms (see Sahni, 1979), nor do they all exhibit arcade-shaped prisms (see Fosse et al., 1978).

5. Surprisingly consistent patterns of enamel ultrastructure were discovered at the subordinal level in multituberculates. With a few interesting exceptions, these results support the hypothesis of Fosse et al. (1978) that taeniolabidoids possess exceptionally large enamel prisms, which serve to distinguish them, as a group, from all other mammals. The few exceptions require further study, however, and may ultimately compel us to reject this hypothesis.

6. Ultrastructural data will likely play an important role in the controversy concerning taeniolabidoid monophyly. A paper discussing the use of enamel ultrastructure in reconstructing multituberculate phylogeny is currently in preparation.

### ACKNOWLEDGEMENTS

We are indebted to D. Baird (PU), W. A. Clemens, Jr. (UCMP), R. C. Fox (UA), P. D. Gingerich (UM), Z. Kielan-Jaworowska (ZPAL), J. A. Lillegraven (UW), M. C. McKenna and M. J. Novacek (AMNH), Chow Minchen (IVPP), B. Slaughter (SMU), and M. Vianey-Liaud (Montpellier) for the loan of specimens for SEM analysis. We have benefited from informative discussion with Drs. W. A. Clemens, Jr., D. C. Fisher, and J. G. Fleagle, and we thank Drs. G. Fosse, P. D. Gingerich, F. E. Grine, and J. W. Osborn for their helpful comments on an earlier draft of this paper. A. R. Biknevicus provided technical assistance and Lucille Betti drafted Figures 3, 6, 10, and 19. This work was supported in part by a Geological Society of America Research Grant to SJC, a Biomedical Research Support Grant from the State University of New York Research Foundation and National Science Foundation grant BSR-84-06707 to DWK, and National Science Foundation grant DEB-82-06242 to Dr. P. D. Gingerich.

## LITERATURE CITED

- BOYDE, A. 1964. The structure and development of mammalian enamel. Unpublished Ph.D. thesis, University of London.
- . 1965. The structure of developing mammalian dental enamel. *In: Tooth Enamel—Its Composition, Properties, and Fundamental Structure* (M. V. Stack and R. W. Fearnhead, eds.; John Wright and Sons Ltd., Bristol):163-167.
- . 1969. Correlation of ameloblast size with enamel prism pattern: use of scanning electron microscope to make surface area measurements. *Zeitschrift für Zellforschung und Mikroskopische Anatomie*, 93:583-593.
- . 1971. Comparative histology of mammalian teeth. *In: Dental Morphology and Evolution* (A. Dahlberg, ed.; University of Chicago Press, Chicago):81-94.
- . 1976. Amelogenesis and the structure of enamel. *In: Scientific Foundations of Dentistry* (B. Cohen and I. R. H. Kramer, eds.; William Heineman Medical Books Ltd., London):335-352.
- . 1978. Development of the structure of the enamel of the incisor teeth in the three classical subordinal groups of the Rodentia. *In: Development, Function and Evolution of Teeth* (P. M. Butler and K. A. Joysey, eds.; Academic Press, New York):43-58.
- , S. J. JONES, and P. S. REYNOLDS. 1978. Quantitative and qualitative studies of enamel etching with acid and EDTA. *In: Scanning Electron Microscopy/1978/II* (R. P. Becker and O. Johari, eds.; SEM Inc., Chicago):991-1002.
- , and K. S. LESTER. 1967. The structure and development of marsupial enamel tubules. *Zeitschrift für Zellforschung und Mikroskopische Anatomie*, 82:558-576.
- , and L. MARTIN. 1982. Enamel microstructure determination in hominoid and cercopithecoid primates. *Anatomy and Embryology*, 165:193-212.
- . 1984. The microstructure of primate dental enamel. *In: Food Acquisition and Processing in Primates* (D. J. Chivers, B. A. Wood, and A. Bilsborough, eds.; Plenum Press, New York):341-367.
- CLEMENS, W. A. and Z. KIELAN-JAWOROWSKA. 1979. Multituberculata. *In: Mesozoic Mammals: The First Two-Thirds of Mammalian History* (J. A. Lillegraven, Z. Kielan-Jaworowska, and W. A. Clemens, eds.; University of California Press, Berkeley):99-149.
- FLYNN, L. J. and J. H. WAHLERT. 1978. Preparation and viewing of rodent incisors for SEM study. *Curator*, 21:303-310.
- FOSSE, G. 1964. The number of prism bases on the inner and outer surfaces of the enamel mantle of human teeth. *Journal of Dental Research*, 43:57-63.
- . 1968a. A quantitative analysis of the numerical density and the distributional pattern of prisms and ameloblasts in dental enamel and tooth germs. III. The calculation of prism diameters and number of prisms per unit area in dental enamel. *Acta Odontologica Scandinavica*, 26:315-336.
- . 1968b. A quantitative analysis of the numerical density and the distributional pattern of prisms and ameloblasts in dental enamel and tooth germs. V. Prism density and pattern on the outer and inner surface of the enamel mantle of canines. *Acta Odontologica Scandinavica*, 26:501-544.
- . 1968c. A quantitative analysis of the numerical density and the distributional pattern of prisms and ameloblasts in dental enamel and tooth germs. VI. The vertical compression of the prism pattern on the outer enamel surface of human permanent teeth. *Acta Odontologica Scandinavica*, 26:545-572.
- , O. ESKILDSEN, S. RISNES, and R. E. SLOAN. 1978. Prism size in tooth enamel of some Late Cretaceous mammals and its value in multituberculate taxonomy. *Zoologica Scripta*, 7:57-61.
- , N.-P. B. JUSTESEN, and G. B. R. WESENBERG. 1981. Microstructure and chemical composition of fossil mammalian teeth. *Calcified Tissue International*, 33:521-528.
- , S. RISNES, and N. HOLMBAKKEN. 1973. Prisms and tubules in multituberculate enamel. *Calcified Tissue Research*, 11:133-150.
- GANTT, D. G. 1977. Enamel of primate teeth: its thickness and structure with reference to functional and phyletic implications. Unpublished Ph.D. thesis, Washington University, St. Louis.
- . 1979. Taxonomic implications of primate dental tissues. *Journal de Biologie Buccale*, 7:149-156.
- . 1980. Implications of enamel prism patterns for the origin of the New World Monkeys. *In: Evolutionary Biology of the New World Monkeys and Continental Drift* (R. L. Ciochon and A. B. Chiarelli, eds.; Plenum Press, New York):201-217.
- . 1982. Neogene hominoid evolution: a tooth's inside view. *In: Teeth: Form, Function, and Evolution* (B. Kurten, ed.; Columbia University Press, New York):93-108.
- . 1983. The enamel of Neogene hominoids: structural and phyletic implications. *In: New Interpretations of Ape and Human Ancestry* (R. L. Ciochon and R. S. Corruccini, eds.; Plenum Press, New York):249-298.

- \_\_\_\_\_. D. R. PILBEAM, and C. STEWARD. 1977. Hominoid enamel prism patterns. *Science*, 198:1155-1157.
- GRINE, F. E. and A. R. I. CRUICKSHANK. 1978. Scanning electron microscope analysis of postcanine tooth structure in the Late Triassic mammal *Eozostrodon* (Eotheria: Triconodonta). *Proceedings of the Electron Microscope Society of South Africa*, 8:121-122.
- \_\_\_\_\_. E. S. VRBA, and A. R. I. CRUICKSHANK. 1979. Enamel prisms and diphyodonty: linked apomorphies of Mammalia. *South African Journal of Science*, 75:114-120.
- HAHN, G. 1973. Neue Zähne von Haramiyiden aus der deutschen Ober-Trias und ihre Beziehungen zu den Multituberculaten. *Palaeontographica*, Abt. A, 142:1-15.
- \_\_\_\_\_. and R. HAHN. 1983. *Fossilium Catalogus I: Animalia*, Pars 127: Multituberculata. Kugler Publications, Amsterdam; 409 pp.
- HOFFMAN, S., W. McEWAN, and C. M. DREW. 1969. Scanning electron microscope studies of EDTA-treated enamel. *Journal of Dental Research*, 48:1234-1242.
- JAFFEE, E. B. and A. M. SHERWOOD. 1951. Physical and chemical comparison of modern and fossil tooth and bone material. U. S. Geological Survey, Report TEM 149:1-19.
- JENKINS, F. A., Jr. and D. W. KRAUSE. 1983. Adaptations for climbing in North American multituberculates (Mammalia). *Science*, 220:712-715.
- KIELAN-JAWOROWSKA, Z. 1974. Results of the Polish-Mongolian Palaeontological Expeditions - Part V. Multituberculate succession in the Late Cretaceous of the Gobi Desert (Mongolia). *Palaeontologica Polonica*, 30:23-44.
- \_\_\_\_\_. 1980. Absence of ptilodontoidean multituberculates from Asia and its palaeogeographic implications. *Lethaia*, 13:169-173.
- KRAUSE, D. W. 1982a. Multituberculates from the Wasatchian Land-Mammal Age, early Eocene, of western North America. *Journal of Paleontology*, 56:271-294.
- \_\_\_\_\_. 1982b. Jaw movement, dental function, and diet in the Paleocene multituberculate *Ptilodus*. *Paleobiology*, 8:265-281.
- \_\_\_\_\_. and F. A. JENKINS, Jr. 1983. The postcranial skeleton of North American multituberculates (Mammalia). *Bulletin of the Museum of Comparative Zoology*, Harvard University, 150:199-246.
- LESTER, K. S. 1971. Fine structure of "fibrils" and tubules in developing opossum enamel. *In: Tooth Enamel*, vol. II (R. W. Fearnhead and M. V. Stack, eds.; John Wright and Sons Ltd., Bristol):63-64.
- MOSS, M. L. 1969. Evolution of mammalian dental enamel. *American Museum Novitates*, 2360:1-39.
- OSBORN, J. W. 1968a. Evaluation of previous assessments of prism directions in human enamel. *Journal of Dental Research*, 47:217-222.
- \_\_\_\_\_. 1968b. Directions and interrelationships of enamel prisms from the sides of human teeth. *Journal of Dental Research*, 47:223-232.
- \_\_\_\_\_. 1968c. Directions and interrelationships of prisms in cuspal and cervical enamel of human teeth. *Journal of Dental Research*, 47:395-402.
- \_\_\_\_\_. 1974. The relationships between prisms and enamel tubules in the teeth of *Didelphis marsupialis*, and the probable origin of the tubules. *Archives of Oral Biology*, 19:835-844.
- \_\_\_\_\_. 1981. Enamel. *In: Dental Anatomy and Embryology* (J. W. Osborn, ed.; Blackwell Scientific Publications, Oxford):174-187.
- \_\_\_\_\_. and J. HILLMAN. 1979. Enamel structure in some therapsids and Mesozoic mammals. *Calcified Tissue International*, 29:47-61.
- PARKER, R. B. and H. TOOTS. 1970. Minor elements in fossil bones. *Geological Society of America, Bulletin*, 81:925-932.
- PEYER, B. 1968. *Comparative Odontology*. University of Chicago Press, Chicago, 347 pp.
- PICKERILL, H. P. 1913. The structure of enamel. *Dental Cosmos*, 55:969-988.
- POOLE, D. F. G. 1967. Enamel structure in primitive mammals. *Journal of Dental Research*, 46:124.
- RIEGER, R. and S. TYLER. 1979. The homology theorem in ultrastructural research. *American Zoologist*, 19:655-664.
- RISNES, S. and G. FOSSE. 1974. The origin of marsupial enamel tubules. *Acta Anatomica*, 87:275-282.
- SAHNI, A. 1979. Enamel ultrastructure of certain North American Cretaceous mammals. *Palaeontographica*, Abt. A, 166:37-49.
- \_\_\_\_\_. 1980. SEM studies of Eocene and Siwalik rodent enamels. *Geoscience Journal*, 1(2):21-30.
- SCOTT, J. H. and N. B. B. SYMONS. 1977. *Introduction to Dental Anatomy*. Churchill Livingstone, New York, 464 pp.
- SLOAN, R. E. 1979. Multituberculata. *In: The Encyclopedia of Paleontology* (R. W. Fairbridge and D. Jablonski, eds.; Dowden, Hutchinson and Ross, Pennsylvania):492-498.
- \_\_\_\_\_. and L. VAN VALEN. 1965. Cretaceous mammals from Montana. *Science*, 148:220-227.
- VAN DER WAAL, I. and L. W. RIPA. 1970. Enamel prism orientation in the cervical region of molar teeth. *British Dental Journal*, 128:282-283.

- VON KOENIGSWALD, W. 1982. Enamel structure in the molars of Arvicolidae (Rodentia, Mammalia), a key to functional morphology and phylogeny. *In: Teeth: Form, Function, and Evolution* (B. Kurten, ed.; Columbia University Press, New York):109-122.
- VRBA, E. S. and GRINE, F. E. 1978. Australopithecine enamel prism patterns. *Science*, 202:890-892.
- WARSHAWSKY, H., K. JOSEPHSEN, A. THYLSTRUP, and O. FEJERSKOV. 1981. The development of enamel structure in rat incisors as compared to the teeth of monkey and man. *The Anatomical Record*, 200:371-399.